PS/HP Note 97-36
revised 11.3.98

CERN - EUROPEAN LABORATORY FOR PARTICLE PHYSICS

FEASIBILITY STUDY OF A DECELERATING RADIO-FREQUENCY QUADRUPOLE SYSTEM FOR THE ANTIPROTON DECELERATOR AD

J. Bosser, P. Bourquin, M. Brouet, B. Couturier, G. Gelato, M. Giovannozzi, F. Grandclaude, J.-Y. Hémery, A.M. Lombardi, U. Mikkelsen, S. Maury, D. Möhl, F. Pedersen, W. Pirkl (editor), U. Raich, H.H. Umstätter and M. Vretenar.

Abstract

This feasibility study reports on a decelerating Radio-Frequency Quadrupole (RFQ) system for post-deceleration of the 100 MeV/c antiproton beam of the AD machine. The corresponding kinetic energy of 5.314 MeV is reduced to values which can be chosen between 10 to 100 keV with minimal blow-up of the normalised beam emittances. This wide range of output energy is required for the second phase of the ASACUSA experiment; it is achieved by electrostatic means.

The study gives details of the overall performance of the system, the proposed implementation of the RFQ, the associated rf equipment, the beam lines, the diagnostics as well as estimations for the cost and the manpower requirements of the project.

Geneva, Switzerland
January 1998

Contents

1. INTRODUCTION

The aim of the study is the conceptual design of a decelerating RFQ able to post-decelerate the antiproton beam of the AD machine from its nominal momentum of 100 MeV/c down to essentially zero. Even ideal adiabatic deceleration, with full conservation of phase space, entails an increase of the physical emittance. The corresponding increase in beam size and/or angle puts severe constraints on the design of the decelerating structure. The design approach of the RFQ described in Section 3.1 leads to a high quality output beam with a very small normalised emittance increase or blow-up.

Compared to the performance of a degrader foil, hitherto used for antiproton 'stopping' experiments, the transmission efficiency of a decelerating RFQ is potentially one to two orders of magnitude higher, and the beam quality is significantly improved. The RFQ concept is therefore of interest for a variety of experiments. The study attempts to devise a flexible design that can be adapted to a wide range of requirements, nevertheless the system presented is fine-tuned to the parameters of the ASACUSA collaboration [1] who have presented firm plans to incorporate the RFQ in later stages of their experiment.

The different phases of this experiment can be summarised as follows:

- phase 1, beginning at startup of the AD machine, will still use a degrader foil at focal point of the beam line DE1. (see layout in annex A):

- phase 2, beginning early in the year 2000, is the first to use the RFQ. A new beam line starts at the former focus of the line DE1, albeit with modified beam profile. The experiment comprises four different set-ups, some of them working with gas targets at pressures up to one Torr. The output energy must be adjustable over a wide range; this critical requirement is met by *electrostatic* post-deceleration. The whole inner structure of the RFQ is mounted on insulating supports to allow application of a variable dc voltage, whereas the tank remains at ground potential. Some consequences of this novel design approach are discussed in paragraph 3.1.4.

  Gas flow is from the experiment to the RFQ; a low-energy beam transport line is needed to focus the beam into the experiment.

- phase 3 foresees a trap mounted in a superconducting solenoid at ultrahigh vacuum. The RFQ output energy is constant. Gas flow is from the RFQ to the trap; no dedicated beam transport line is needed since the solenoid field "pinches" the beam very efficiently.

"End-to-end" simulations, from the "handover" point to the entrance of the experiment, are given in Section 4 for the representative conditions of phases 2 and 3. The project planning for the implementation of the RFQ and estimates for cost and manpower complete the study report.

2. KEY PARAMETERS

Input beam:

Unless otherwise noted, the parameters refer to the "handover" point, i.e. the plane of beam focus for ASACUSA phase 1.

Momentum	p = 100 MeV/c	(T = 5.314 MeV, β = 0.10598)
Repetition period	70 to 100 s	

Longitudinal parameters:

Bunch shape and energy spread are both taken to be Gaussian and can be adjusted within wide limits by the bunching voltage of the 176 kHz system in the AD machine. Typical figures are given below. They are expressed in 5σ values (from -2.5σ to +2.5σ of the distribution, i.e. containing 95.6% of particles of the bi-Gaussian distribution, 98.7% in its one-dimensional projection).

Bunching voltage [V]	Full bunch length (5σ) [ns]	Full energy spread (5σ) [keV]
100	730	7.5
500	487	11.5

Transverse parameters:

Emittance (each plane, 2σ definition, $\varepsilon_{x,y} = (2\sigma_{x,y})^2 / \beta_{x,y}$, i.e. containing 86.5% of particles in each plane for Gaussian distribution, unnormalised, at handover point):

$\varepsilon = 1\pi$ mm•mrad (nominal)
$\varepsilon = 5\pi$ mm•mrad (initial)
$\varepsilon = 10\pi$ mm•mrad (initial "effective overall" envelope, see paragraph 3.4)

TWISS parameters:

	At handover point	At input of RFQ
α_h	0.13	0.92
β_h [m]	7.55	0.44
α_v	3.30	0.92
β_v [m]	0.72	0.44

Output beam:

The performance quoted in the following are for a beam with nominal input parameters and "effective overall" emittance equal to 10π mm•mrad. All the incoming particles with

nominal input parameters at the handover point are transmitted through the system, however only the fraction accepted by each of the experiment has been quoted.

At the RFQ output plane:

Energy: adjustable between 10 keV and 100 keV
Time structure:

- microstructure (bunches) 5 ns, structure rapidly decreasing in output line,
- macrostructure: envelope same as at input, non-decelerated particles precede particles of nominal output energy by ~84 ns.

Fraction of the incoming particles that are decelerated to any energy of choice:

Within ±10 keV	50%
±5 keV	47%

At the formvar window for ASACUSA phase 2, (target experiment):

Fraction of the incoming particles decelerated to 50 ±5 keV and delivered to the experiment:

Within a spot size of 5 mm diameter	44%
Within a spot size of 6.5 mm diameter	47%

In the middle of the SC solenoid for ASACUSA phase 3 (trap in SC solenoid):

Fraction of the incoming particles trapped in a 50-cm-long trap placed 1 m downstream of the RFQ, in a 5 T solenoidal field, as specified in Ref. [1] and subsequent private communication.

Within a spot size of 3 mm diameter	41%
Within a spot size of 4 mm diameter	43%

Detailed beam characteristics are reported in Chapter 4 (End-to-end simulations).

3. DESCRIPTION OF THE CHOSEN STRUCTURE

3.1 RFQ

3.1.1 General

Five solutions (see Appendix C) were studied and taken into consideration to fulfil the experimenters' requirements for phase 2 and 3. Finally the so-called "electrostatic" solution has been retained for its simplicity and flexibility. It is also the only one which allows energy correction before the RFQ deceleration process begins.

The RFQ decelerating system is composed of three parts (see Figure in Appendix B):

- ***The medium-energy beam transport line (MEBT)***: It is composed of two quadrupoles and two horizontal/vertical steering dipoles for transverse matching and steering, together with two identical rf cavities for the matching in the longitudinal phase space. The first cavity imprints an energy modulation on the beam (which after the drift space results in the required density modulation or "bunching"), the second permits correction of the average beam energy at the input of the RFQ (in particular the compensation of the dc potential difference between the RFQ cover and the inner structure).

- ***The RFQ***. It decelerates the 5.314 MeV (100MeV/c) antiproton beam to 50 keV. The inner structure of the RFQ is mounted on ceramic insulators and can be raised to a dc voltage of ±50 kV, allowing for the "electrostatic" output energy variation in the range 10 to 100 keV. The RFQ output energy of 50 keV has been chosen in order to get direct compatibility with phase 3 requirements of ASACUSA. The energy range for phase 2 may be extended by providing higher RFQ output energy and an accordingly increased dc voltage range at the inner RFQ structure.

- ***The low-energy beam transport line (LEBT)***. It consists of three independent quadrupoles to focus the beam on to the physics experiment, together with a short straight section to accommodate diagnostics.

The choice of 202.56 MHz as the resonant frequency for all the rf elements involved in the set-up is the result of a compromise. Efficiency of beam-structure interaction favours lower frequencies, however at the cost of a dramatic increase of the total length (a 100 MHz system would be almost twice as long).

The RFQ is a linear accelerating/decelerating structure differing from other linear structures by the fact that the active part consists of 4 electrodes (called rods or vanes) which are placed *parallel* to the beam. They create a transverse (xy-) electric quadrupole field providing alternating gradient focusing of the beam by an rf-voltage. The longitudinal field component, generated normally by drift tubes or irises, is produced in the RFQ by depth modulation of the electrodes (see Figure 1). Its extent is determined by the modulation factor *m*. Peaks in one plane correspond to troughs in the other.

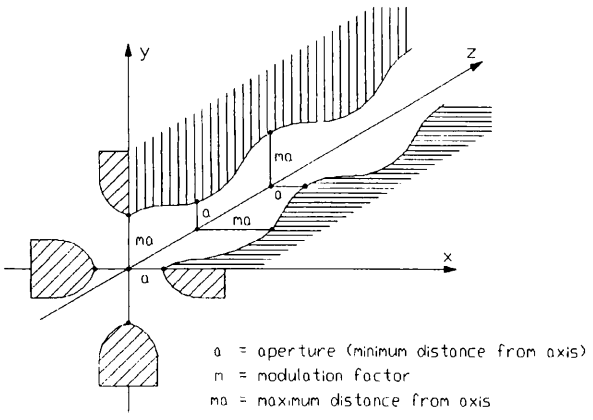

Figure 1 - Schematic view of the RFQ electrodes

The modulation of an electrode along the RFQ is shown in Figure 2. The distance between subsequent peaks (or troughs) is equal to the length the beam travels during one rf period. Since the velocity of the beam is reduced by a factor of ~10 during the deceleration, the longitudinal width of the modulation is reduced accordingly.

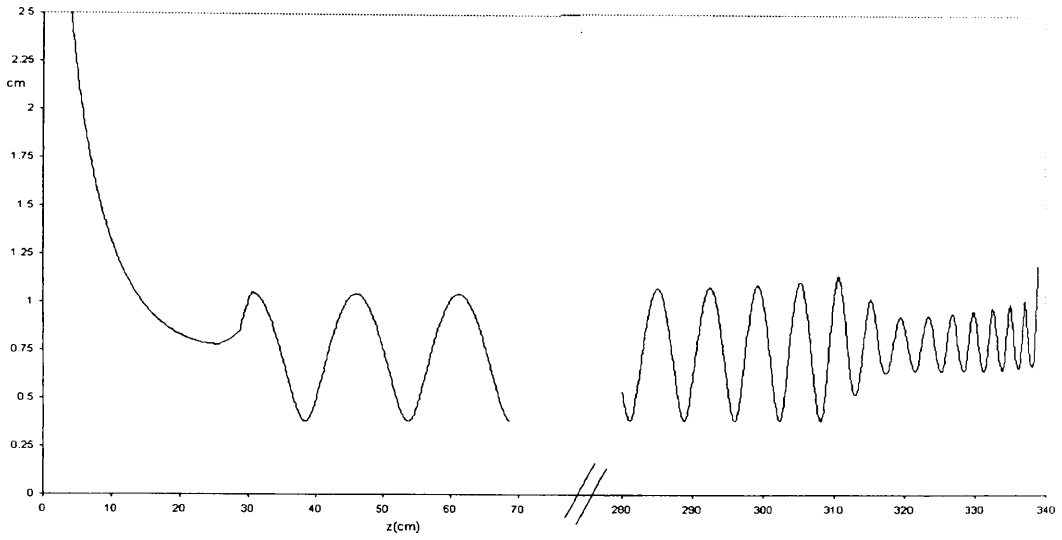

Figure 2 - Profile of RFQ electrode with different modulation widths at high-energy input (left) andlow-energy output(right), accommodating the reduction in beam velocity during deceleration

3.1.2 Beam dynamics

It is the longitudinal beam dynamics that dictate the RFQ design. In fact, contrary to a conventional accelerating RFQ where careful shaping and smooth adiabatic bunching at low energy permits efficient beam capture, a completely different longitudinal dynamics scheme had to be implemented. The main differences with respect to a conventional accelerating RFQ are:

- adiabatic bunching at high energy leads to prohibitive RFQ length. In an accelerating RFQ about 2/3 of the total length may be devoted to bunching. This proportion becomes unmanageable for the much longer cell dimensions at the high energy end.

- the longitudinal stable area for a given RF voltage is reduced in size during deceleration. In parallel the requirements for transverse focusing increase, since the *physical* beam emittance grows due to the adiabatic blow-up, even if the *normalised* emittance is preserved.

In order to overcome these problems, a *discrete* bunching is performed before injection into the RFQ. This is the main limiting factor in the overall transmission of the proposed layout, since a single buncher can only put a limited percentage of the beam into the

longitudinal acceptance of the RFQ, which then decelerates that fraction to the low output energy with virtually no loss.

The characteristics of longitudinal matching were determined by backtracking from the critical low energy end. The bunching voltage and consequently the distance between the buncher and the RFQ are determined by the longitudinal bucket size at the low energy end. The trade-off between required minimum longitudinal bucket size and transverse focusing along the structure has then been optimised within the limits of permissible rf field strength and electrode modulation, taking machining constraints into due account.

The global characteristics of the RFQ and rf cavities are summarised in Table 1. The relevant characteristics along the RFQ, namely minimum radius of aperture, vane modulation and synchronous phase are given in Figure 3. The beam envelope and the beam input and output phase plane are given in Figures 4 and 5.

Table 1. Global characteristics of RFQ and RF cavities

PRE-BUNCHER/CORRECTOR CAVITIES	
Frequency:	202.56 MHz
Effective voltage:	50 kV
Aperture radius:	15 mm
Length:	300 mm
RFQ	
Frequency:	202.56 MHz
Vane voltage:	167 kV
Maximum electric field:	33 MV/m (corresponding to 1.8 Kilpatrick)
Vane length:	340 cm
Number of beam dynamics cells:	76
Power losses:	700 kW (rough estimate)
Average radius of aperture:	0.79 cm
Minimum radius of aperture:	0.4 cm
Vane modulation factor (max.):	2.9
BEAM RELATED PARAMETERS *)	
Transverse design emittance:	10 π mm mrad
Transverse acceptance **):	15π mm mrad
Design energy spread:	$\pm 0.5 \times 10^{-3}$
Energy spread acceptance **):	$\pm 0.9 \times 10^{-3}$
Transverse normalised-emittance growth:	~0 (within simulation accuracy)
Transmission:	47%
(input beam with design parameters, output beam for phase 3, into ±5 keV)	

*) Output parameters: total count, within quoted limits, of macroparticles used for tracking simulation
**) Transmission unchanged, max. emittance increase 10%, all input parameters supposed nominal.

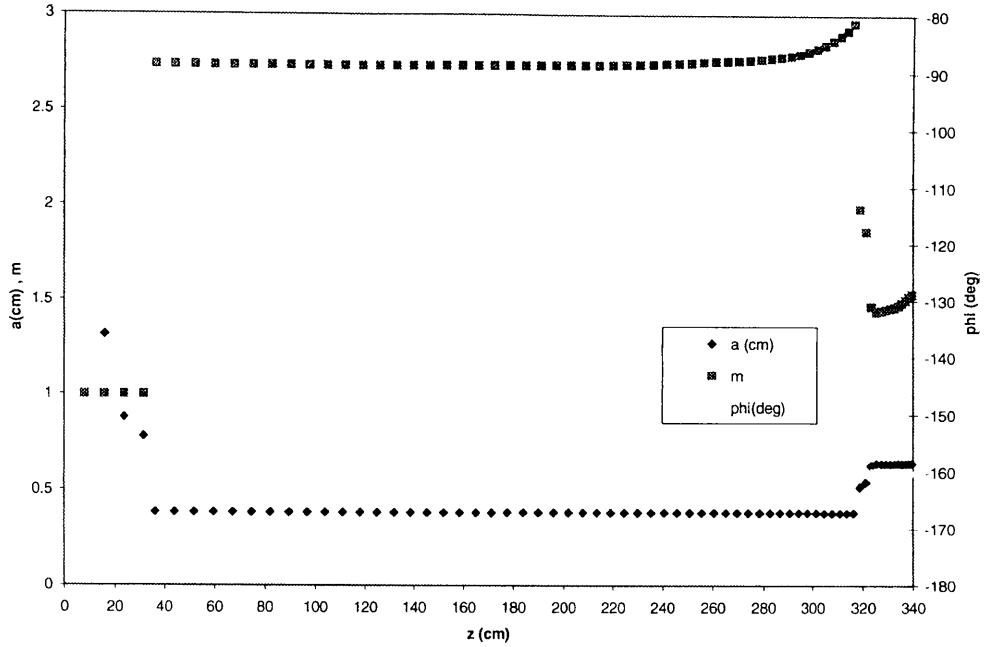

Figure 3 - Minimum aperture (a), modulation (m) and synchronous phase (phi) vs. length

It should be noticed that these data are based on a transverse emittance of 10 π at the input of the RFQ. This is realistic for first-time operation where random errors of beam position etc. may increase the "effective overall emittance "(i.e. the area of phase space where a given fraction, say 95%, of the beam is found). In later phases of AD operation this input emittance may be reduced by an order of magnitude. On the other hand, the different definitions of particle populations at input and output may result in slightly optimistic figures.

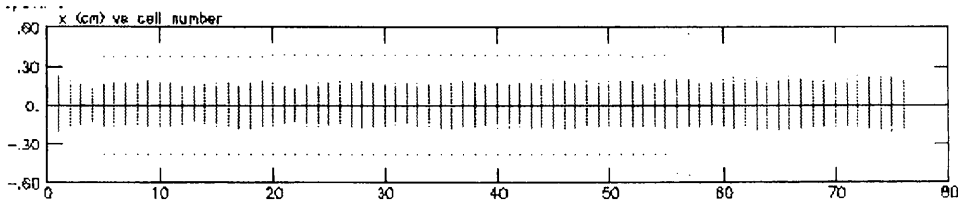

Figure 4 - Beam envelope (cm) vs. cell number (PARMTEQM results)

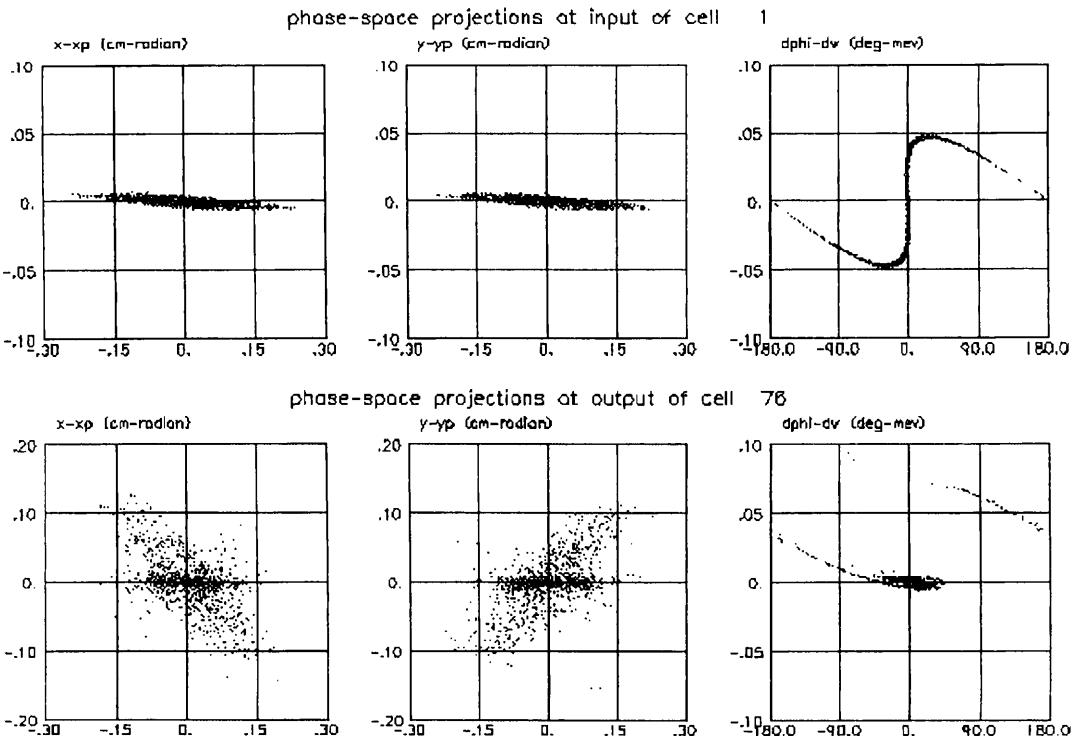

Figure 5 - RFQ input (top) and output (bottom) phase space. Left column: Horizontal plane Middle column: vertical plane. Right column: Longitudinal plane(PARMTEQM results)

Conservation of *longitudinal phase* space leads ideally to conservation of the *absolute* energy spread presented at the input of the buncher. This is the dominant part of the overall output energy spread, as the intrinsic blow-up in the RFQ is small. Additional contributions due to external fluctuations are negligible, since on the one hand the output energy of the RFQ is in first approximation independent of rf power level (and its possible instabilities), on the other hand the stability of the dc supply used for post-deceleration is orders of magnitude above any critical limit.

The effect of element fluctuations in the *transverse* phase space is discussed in Section 3.4 (Beam Lines).

3.1.3 Mechanical Engineering

Basic principles

The vacuum tank and the electrode support are independent elements. The assembly of the electrodes on their support is made outside the tank.

The support or "girder" is fixed on a surface table in the same configuration as that foreseen in the tank, the electrodes are then put in place. The position tolerance between the electrodes is ±0.04mm and the straightness tolerance is ±0.1mm/3415mm. Manufacturing tolerances are sufficiently tight to allow mounting of the electrodes without shims.

The completed girder/electrode assembly is then rolled into the tank and put on its insulating supports. These supports are made of alumina (high purity aluminum oxide ceramic). To avoid flexion and shear stresses in the ceramic, the electrode support has been mounted vertically. This position, although not optimal for RF symmetry, permits nevertheless a satisfactory rf field pattern.

No dedicated cooling is provided since the nominal average power dissipation for the antiproton pulse rate is only a few watts. It may however be desirable to provide interleaving rf test pulses at rates up to two orders of magnitude higher. Several engineering possibilities exist to dissipate the increased heat load if the higher rf repetition rates are adopted.

The sighting line is fixed with respect to the entry and exit centre line of the electrodes. This is transferred as a reference to the exterior by two targets and a transverse level.

Three alignment jacks allow the positioning of the completed RFQ.

The design allows the rapid change of electrodes if necessary. The total duration for the manufacture and mounting of one set of electrodes is estimated at about three months.

Vacuum tank

The vacuum tank is a tube of 380 mm inside diameter (precision ±0.5mm) and 3415 mm length. It is made from 15 mm thick sheet of Cr.Ni.18-10 (Inox 304L). All the flanges are in Cr.Ni.18-12 Mo.N. (Inox 316L+N). They are CF type except for the main covers which are for metal toroïdal joints. All the pieces have to be vacuum fired at 950°C for Ultra-High Vacuum.

Electrode Support

The electrode support, comprising 34 cells, is made of OFE Cu. The assembly takes the form of a ladder, where the rungs serve as supports for the electrodes. All machining is done before the final assembly. Assembly is completed by brazing under vacuum 3 lengths of about 1350 mm. These 3 parts are then mechanically assembled. The ladder assembly is insulated and supported inside the tank on 3 points and restrained by 2 upper points reproducing the support conditions that have served outside for mounting the electrodes.

Electrodes

The electrodes are made from 1000 mm lengths of OFE 4/4 (hard) copper bars. The transverse profile is obtained by planing and the longitudinal modulation by numerically controlled machining using profiled milling cutters.

The electrode parts are fixed to the support by one central dowel pin and screws in stainless steel. The contact between electrodes and their support is achieved with the aid of commercial rf finger contacts. They do not interfere with the positioning of the electrodes. The contact between electrode lengths remains to be defined.

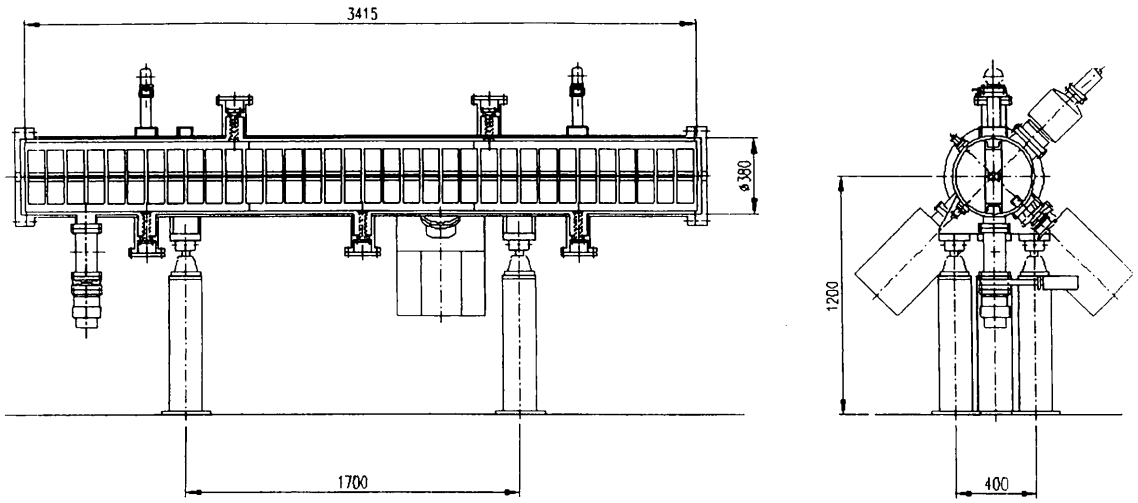

Figure 6 - Sectional view of RFQ with ladder structure of 34 rf cells

3.1.4 RF aspects

Choice of resonating structure

The so-called "4-rod" structure has been retained since it allows easy exchange of the electrodes and also avoids dipole excitation problems that plague the "4-vane" structure. It consists of 34 coupled cells of equal length (0.1 m) resonating at 202.56 MHz.

Three types of 4-rod structures inside a cylindrical tank have been studied, differing by the way in which the positive and negative poles of the rf-voltage are connected to the rods:

- the "ladder" structure in which the rods are connected by two stems towards a top girder and towards a bottom girder (stems forming the rungs of a ladder),
- the "comb" structure in which the supporting stems are fixed to only one girder on the bottom (resembling a comb),
- a third structure in which the stems are replaced by irises or discs with the four rods passing through the central window of all irises.

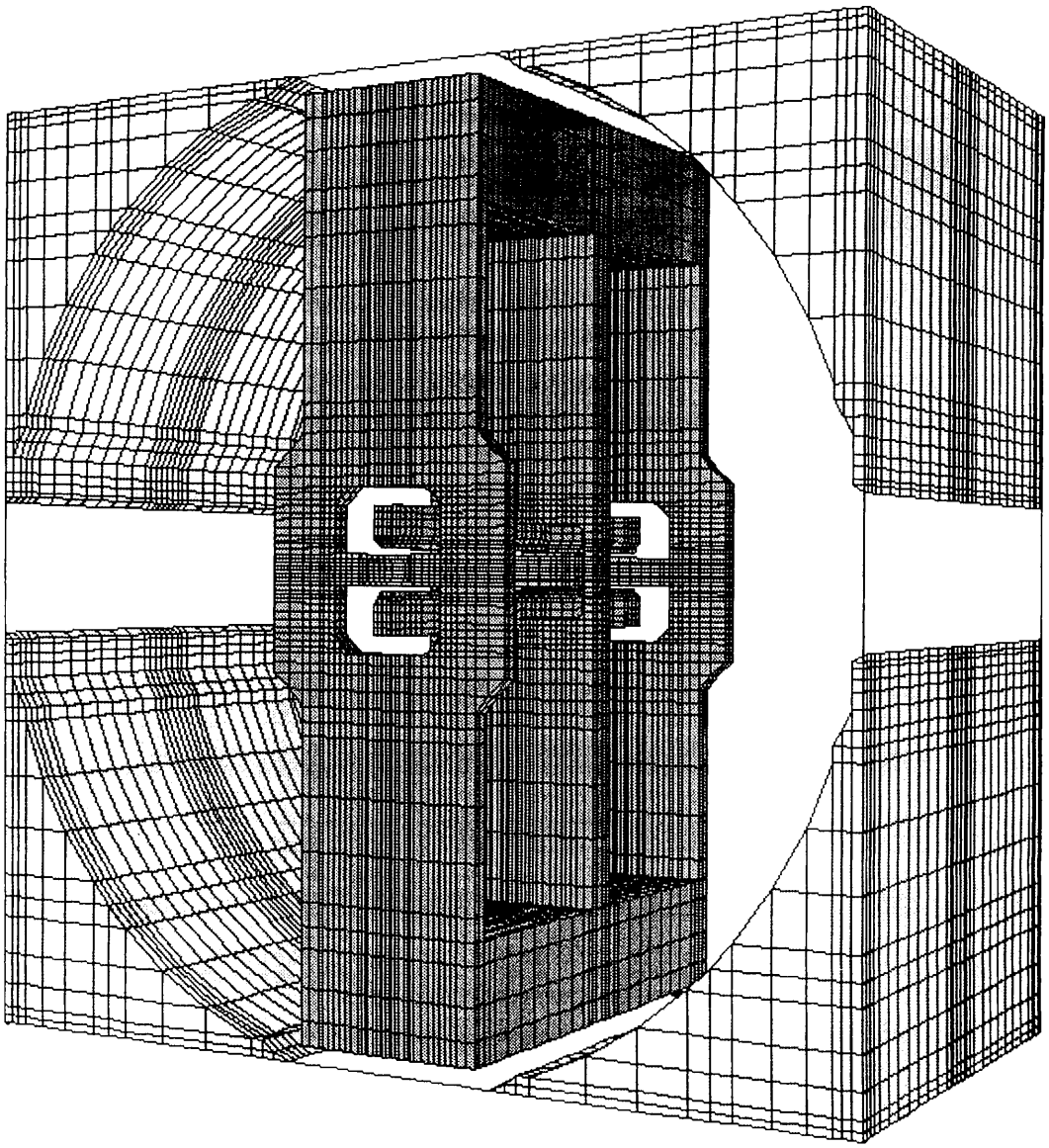

Figure 7 - Finite element mesh used for electromagnetic field computation. It shows a cross section through the cylindrical tank and 3 rungs of the "ladder structure", i.e. 2 out of 34 subsequent "RF-cells" (cf. Figure 6). The 4 RFQ-electrodes are visible in the central windows. (MAFIA result)

As a result of MAFIA computations, the comb structure was discarded in favour of the ladder structure because the top-bottom asymmetry in voltage yields a small undesired deflection field superposed on the quadrupole field. The "ladder" solves this symmetry problem and gave good results in the previously built RFQ for LIS (Laser Ion Source). The "disc" structure leads to better Q-values, but was not compatible with the requirements of the electrostatic post-deceleration, since the closed geometry virtually precludes inductive coupling. Thus the ladder structure was chosen.

In order to accomplish an additional, variable deceleration at lowest energy by the electrostatic potential difference between the rods and the outlet of the tank it is necessary to put the whole resonating structure on a variable, high-voltage potential. Figure 7 above shows two cells of the isolated ladder structure in finite element representation.

The assembly of girders, stems and electrodes (dark colour) floats electrically within the tank. The dc decelerating voltage is connected from outside via a HV feed-through, while rf power and rf diagnostics are coupled inductively to the assembly. Its stray capacitance to the inside tank provides the rf connection which can be enhanced by additional "flaps" (not shown). Note the different geometry of subsequent stems. This serves to reduce a small voltage difference in subsequent windows which results from the fact that the stems are mounted vertically (for mechanical reasons) and not at 45 degrees (which would provide the best rf symmetry for the electrode connections).

The computed Q-factor for this structure with a copper ladder in a stainless steel tank is 9900. Experience has shown that the practically achievable Q-factor is considerably lower.

Undesired modes and dispersion relations

A set of *two* rf cells is the basic building block in this bi-periodic structure where alternate cells work with opposite phase. The RFQ operates at the "cut-off" frequency of the basic cell mode where the phase difference between 2-cell blocks is zero. The overall resonant frequency of the standing wave in the tank is then identical to the cut-off frequency of the cells, and independent of the tank length.

At frequencies higher than cut-off the phase difference between 2-cell blocks increases according to the hyperbolic "dispersion" relation. Additional standing-wave resonances occur where the total unidirectional phase advance in the tank is a multiple of π. They depend on the number of cells and may perturb operation if too close to the operating frequency. Figure 8 shows the dispersion curve for a 2 * 20 cell ladder in units of $\pi/20$, i.e. the phase increments meeting this resonance condition. The first longitudinal resonance lies 2.58 MHz above the operating frequency, corresponding to about 250 half-bandwidths at the full theoretical Q-factor. This assures separation in excess of 30 dB even if the practical Q-factor is 3 times inferior. The fact that the tank comprises only 34 rather than 40 cell is an additional safety factor.

Parallel studies with the circuit-analysis program PSPICE using an equivalent lumped circuit model of the resonator chain have confirmed that the longitudinal field flatness can be held within a few percent.

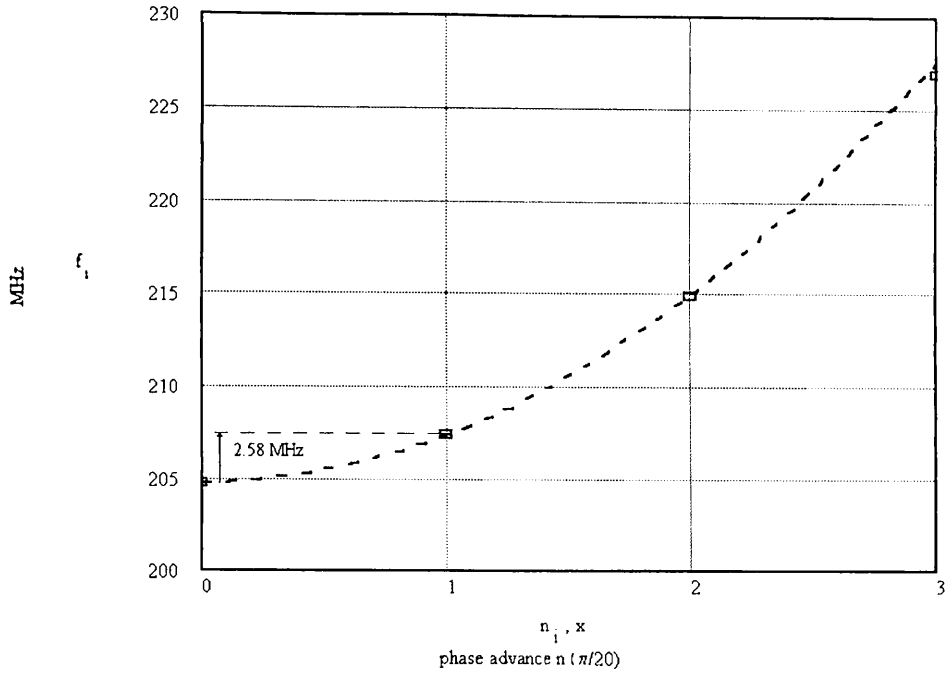

Figure 8 - Dispersion curve of the accelerating RF-structure

The dc isolation of the ladder structure from the tank leads to the existence of unwanted modes with an electric field between girders and tank wall (the TEM- and the first circumferential TE-mode). Their frequencies lie mainly below the operating frequency and can be varied by the capacitance between girders and tank. These modes can easily be damped. Also their coupling with the operating mode is minimised by the choice of an *even* number of rf cells to cancel the overall effect of individual couplings at alternate phases.

Higher order modes (HOM) of the individual cell geometry are much higher in frequency (480 MHz) and can be selectively damped if necessary.

In spite of the important length of the RFQ and the requirements of electrostatic deceleration the proposed design is robust and will in all probability not present unusual difficulties for its implementation.

3.2 Buncher and Corrector Cavities

Two structures have been studied

- pillbox cavity with single gap and nose cones. This is the standard implementation for high-current machines.
- coaxial TEM resonator loaded with double gap. This kind of approach using multiple gaps is increasingly popular, especially for low-velocity beams.

The program SUPERFISH was used for the comparative analysis. For the TEM resonator the double gap capacitance was first evaluated by the POISSON code and then converted into an equivalent geometry with cylindrical symmetry.

The requirements and the results are resumed in Table 2 below.

Table 2. Comparision TEM vs. Pillbox cavity characteristics

	TEM	Pillbox
Frequency	202.56 MHz	
Beam wavelength ($\beta\lambda$)	15.7 mm	
Gap length	40 mm	
Aperture radius	15 mm	
Nominal beam peak voltage ($U_{B)}$	50 kV	
Transit Time Factor (T)	0.75	
Number of gaps (n)	2	1
Cavity voltage ($U_C = U_B/(T\ n)$	33.33 kV	66.67 kV
Cavity breakdown voltage (Kilpatrick=1)	313 kV	246 kV
Quality factor Q (Cu 100 %)	10 744	18 300
Shunt impedance $r = U_C^2/(2P)$	1.05 MΩ	0.645 MΩ
Characteristic impedance r/Q	97.7 Ω	35.2 Ω
Nominal power P (Cu 100 %)	0.528kW	3.45 kW

Considering the more than 6-fold reduction in required amplifier power, the TEM structure with double gap is clearly preferable. Its considerably higher characteristic impedance has no noticeable disadvantage in the present low-current application. The large margin with respect to breakdown voltage, as well as the rf power available from standard semiconductor amplifiers, provide ample reserve to increase the voltage in the energy corrector cavity if necessary. In addition the mechanical layout is simpler and more compact.

The TEM structure with double gap has therefore been retained for both cavities.

3.3 RF Equipment

The rf system for the decelerating RFQ facility is composed of three rf chains at 202.56 MHz. Two identical 4.5 kW chains are used for the buncher and energy corrector, and a 750 kW chain for the RFQ.

The rf pulse length is determined by the cavity filling time, which is much longer than the beam pulse length. Considering for the RFQ a maximum unloaded Q-value of 10'000 (Q will be lower for buncher and energy corrector), the time to reach 99% of the voltage (without the amplitude servo system) would be 115 μs. With a safety margin, the maximum rf pulse lenth can be taken as 150 μs. For stability reasons, it would be preferable to pulse the system at 1 Hz (as in most CERN linacs) even if the beam has a much lower repetition rate. The rf duty cycle would be only 0.15 ‰.

For the power levels and duty cycles required we propose to use the standard CERN linac rf architecture. The use of such a well-proven design would also allow the recuperation of some equipment dismantled from the old Linac1. However, in this case some consolidation work would be necessary, to have a reliable system with minimum intervention times. The phase and amplitude stabilisation system used in Linac2 (Fig. 9) has a phase stability of ±1° and amplitude stability of ±1%. This is considered as sufficient for the AD RFQ facility. The phase shifter design of Linac2 has a 2.8° resolution in the phase adjustment between the cavities, but in case a higher resolution is needed, one can use the (more expensive) 0.5° resolution phase shifter design of Linac3.

Figure 10 shows the proposed layout of the rf system. The amplified signal of the master oscillator is split in four, feeding the three rf chains (one output is available for phase reference). The three chains have an identical amplifier stage at 4.5 kW output power. The RFQ chain has two additional amplifier stages, a first up to 60 kW (it can be of the "Frank James" type used at the CERN linacs), and a final stage delivering a power of 750 kW. The latter can use a re-constructed Linac1-type amplifier. The 35 kV anode voltage for its tube is provided by a dedicated power supply.

In case the Q-value of the RFQ would be lower than foreseen, the option of upgrading the installation with an intermediate stage before the Linac1-type amplifier is left open. This can consist of a "Siemens" amplifier as used in Linac1 and could use the same high voltage supply as the final amplifier, raising the final power to 1.2 MW.

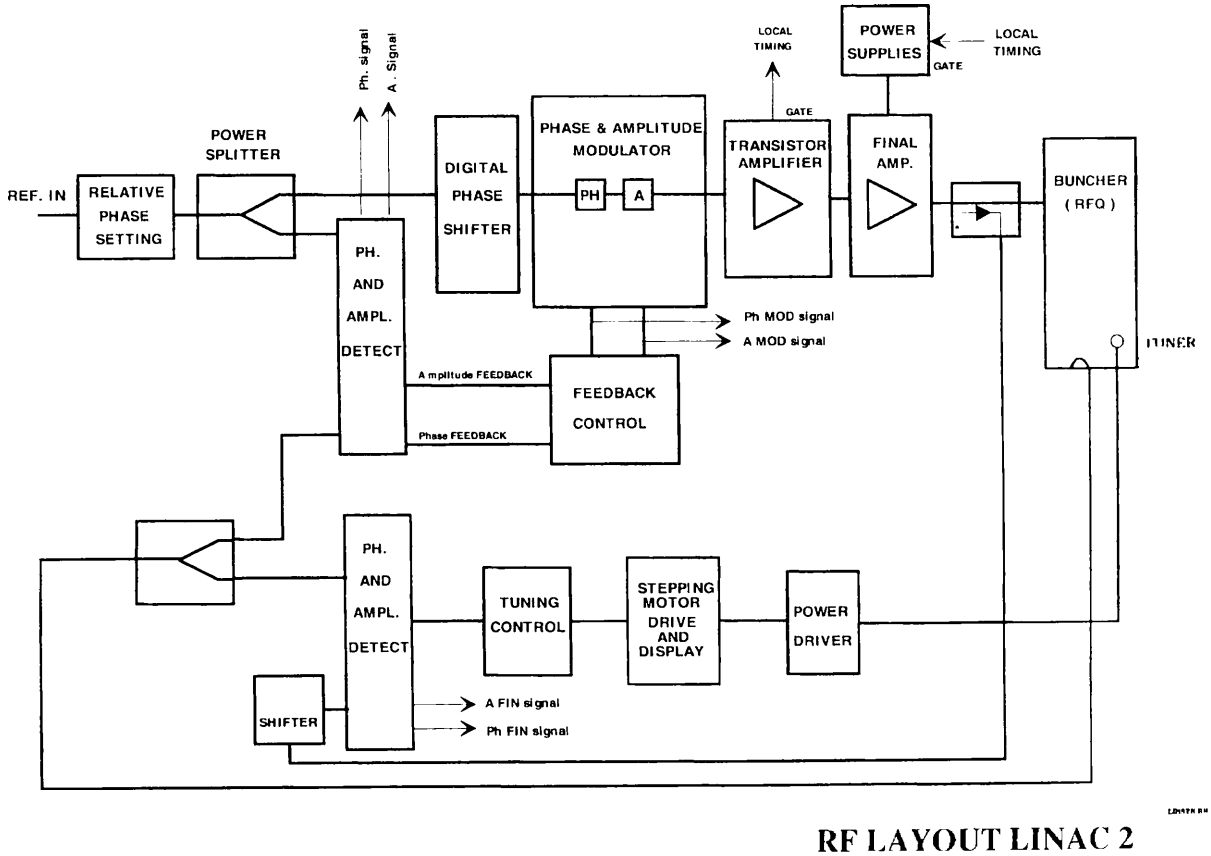

Figure 9 - Standard CERN phase and amplitude regulation loops

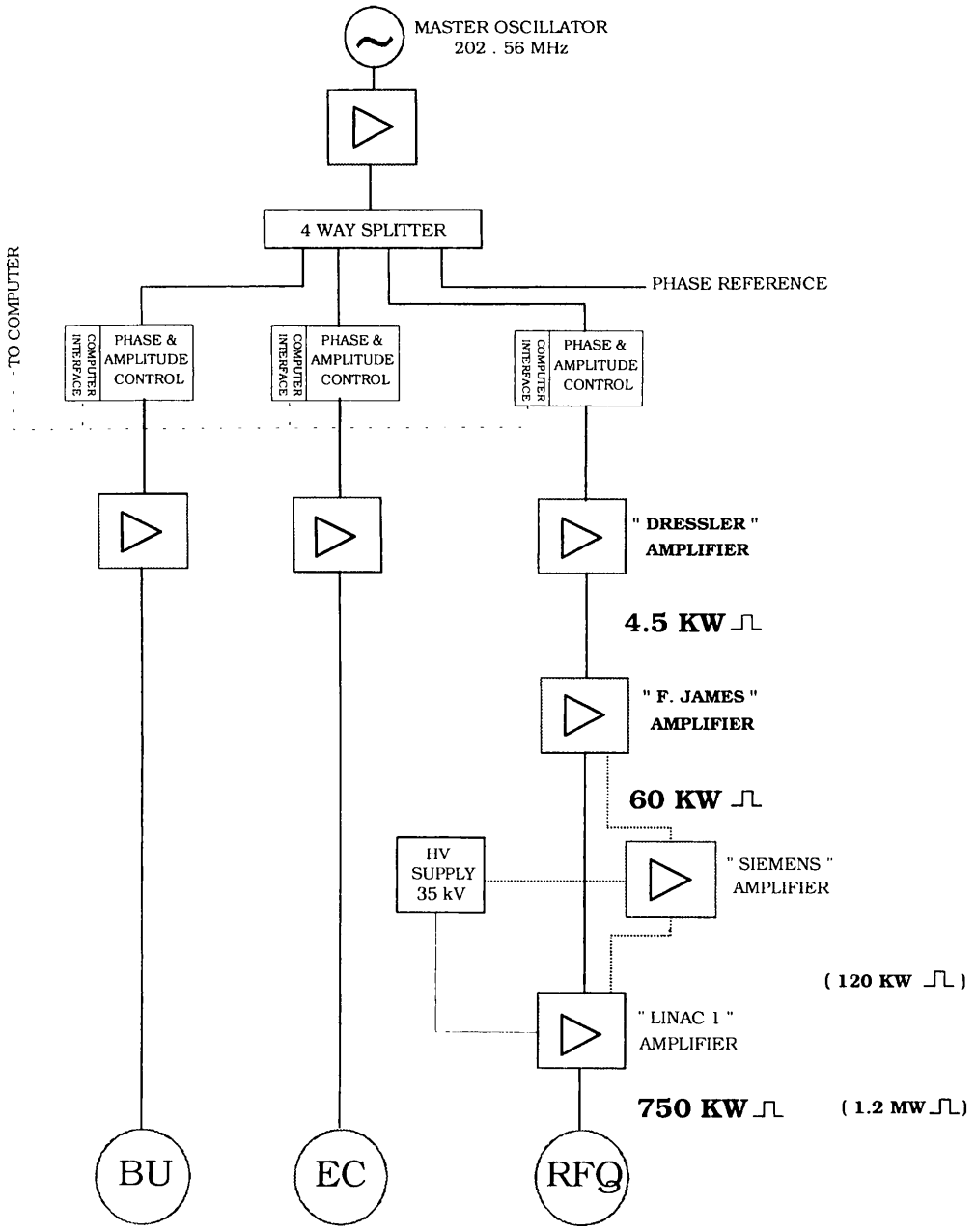

Figure 10 - Layout of the rf system for the RFQ, the buncher (BU) and the energy corrector (EC)

3.4 Beam Lines

3.4.1 Medium Energy Beam Transport (MEBT)

To transport antiproton beams from the handover point to the RFQ, a dedicated straight section of beam line has been studied. This line will be connected to the transfer line normally used by the ASACUSA Collaboration during the first period of data taking.

The first element encountered by the antiprotons is the buncher, then a drift of 6.15 m allows the beam to rotate in the longitudinal phase space in order to have the correct parameters at the entrance of the RFQ. The constraints for the optics are the following:

- at the entrance to the buncher the beam should have a maximum size of 10 mm (radius), in order to reduce the distortions of the electromagnetic fields generated by larger apertures;

- at the entrance of the RFQ the optical parameters should have the values in Table 3:

Table 3. Optical parameter at the entrance of the RFQ

α_H	β_H [m]	α_V	β_V [m]
0.92	0.44	0.92	0.44

- the dispersion function D_H and its derivative D_H' should be zero all along the transfer line. This condition is necessary to avoid beam blow-up due to the momentum spread of $\pm 5 \times 10^{-3}$, corresponding to 95% of the particles, generated by the buncher.

Three different optics have been computed. A complete analysis, including a sensitivity study with random errors, has been carried out using the program MAD. The solution retained is obtained by modifying the optics upstream of the buncher and using two quadrupoles installed between the buncher and the RFQ (see Annex B for a schematic view of the transfer line). The values of the optical functions are shown in Figure 11 from the extraction septum of the AD machine to the entrance of the RFQ.

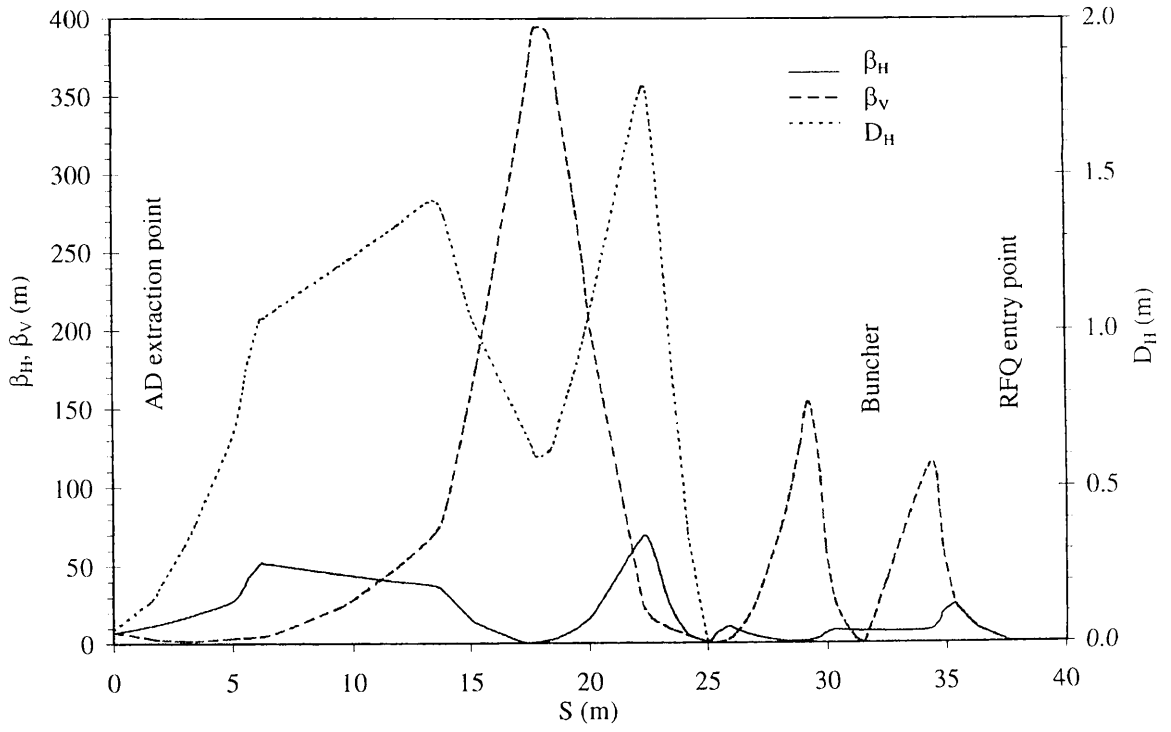

Figure 11 - Optical functions for the transfer line from the extraction septum of the AD machine to the entrance of the RFQ

[The centre of the buncher is placed at S = 31.41 m]

Figure 12 shows the beam envelope downstream the hand-over point (the centre of the buncher), which has been chosen as reference point for the *S*-coordinate.

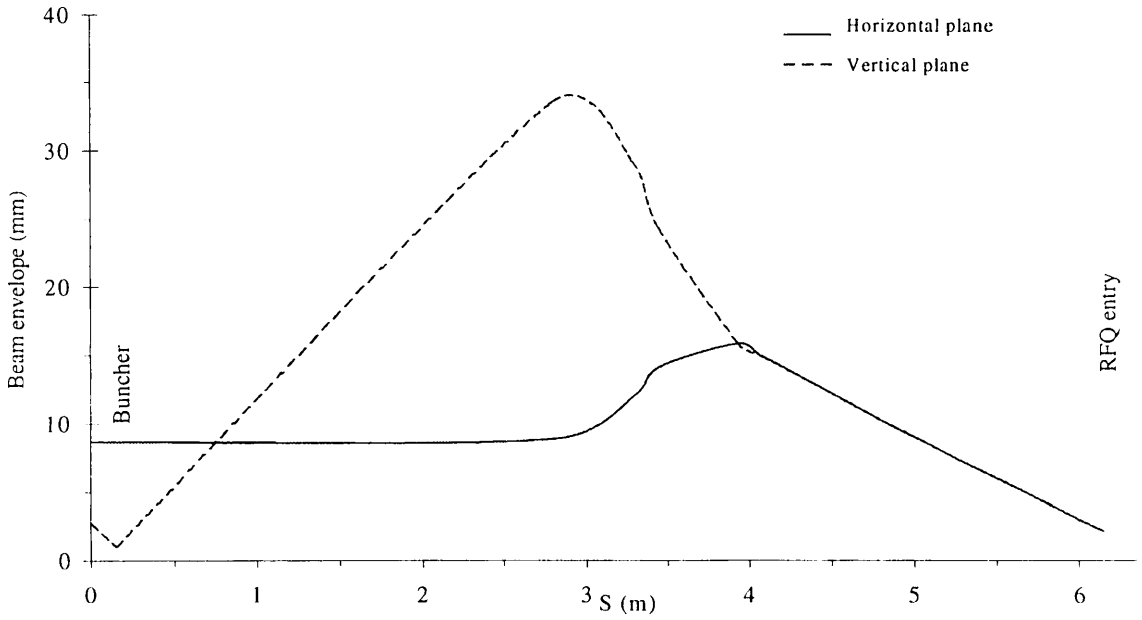

Figure 12 - Evolution of the horizontal and vertical beam radius from the centre of the buncher to the entrance of the RFQ
[The beam radius is computed using the effective overall emittance of 10π]

To fulfil the constraints at the location of the buncher, the beam is parallel in the horizontal plane, while it is focused in the vertical plane. The values of the optical parameters at the buncher location for the nominal optics are given in Table 4.

Table4. Optical parameter at the centre of the buncher

α_H	β_H [m]	α_V	β_V [m]
0.13	7.55	3.30	0.72

The beam radii at the same location can be computed immediately, and are given in Table 5.

Table 5. Beam radii at the centre of the buncher

$\varepsilon_H = \varepsilon_V$ [mm mrad]	r_H[mm]	r_V[mm]
1 π	2.7	0.8
10 π	8.7	2.7

The two values of the emittances represent two extreme situations: 1π is the nominal beam emittance [2], while 10π is an effective overall emittance. This quantity represents the surface in phase space covered by the beam over successive shots. The effective overall emittance allows to take into account the effect of different perturbing effects, such as extraction errors, power supply instabilities, calibration drifts etc., which would produce shot-to-shot fluctuations of the beam parameters. Preliminary studies on the model of the AD machine, have shown that 10π is a realistic value for the effective overall emittance. From the values quoted, one can state that an aperture of 15-20 mm radius is necessary for the buncher to avoid a bottleneck.

In addition to the two quadrupoles, four steering magnets have been foreseen for installation in the beam line. The complete magnet equipment list is shown in Table 6:

Table 6. Magnetic elements to be installed in the beam line [The corrector magnets are combined in order to have two steering elements combining horizontal and vertical deflection]

Description	Name	Power supply	Current Limit [A]	Power supply resolution	Availability
quadrupole	Q42.13	L 10.25	10	$< 10^{-3}$	yes
quadrupole	Q42.14	L 10.26	10	$< 10^{-3}$	yes
corrector	DipB28a02h	L 10.28	10	$< 10^{-3}$	yes
corrector	DipB28a02v	L 10.29	10	$< 10^{-3}$	yes
corrector	DipB28a03h	L 10.30	10	$< 10^{-3}$	yes
corrector	DipB28a03v	L 10.31	10	$< 10^{-3}$	yes

A key parameter in the definition of the transfer line characteristics is the transmission efficiency. In order to estimate this quantity, a number of dedicated simulations have been performed. The approach to the problem is to introduce realistic errors in the beam line model and to verify whether the beam parameters are still in the nominal acceptance of the RFQ (15π). Errors on the three bending magnets and nine quadrupoles downstream of the magnet ATP.BHZ8000 have been considered. Furthermore, uniformly distributed, non-correlated errors with an amplitude of $\pm 10^{-3}$ relative to the nominal value of the specified magnetic element have been assumed. It should be noted that a relative error of 10^{-3} on the dipole settings corresponds to a variation of the magnetic field of only 2.6×10^{-4} T·m.

With this choice for the parameters used in the simulations, it turns out that the effective overall emittance at the location of the buncher is $\approx 10\pi$. In the simulations, 5000 samples of the random errors have been generated. The results are summarised as follows:

- the residual horizontal dispersion function does not exceed ±40 mm at the RFQ entrance as well as all along the transfer line. Therefore, no significant beam blow-up due to the momentum spread generated by the buncher is expected;

- the residual trajectory error is less than 1 mm at the RFQ entrance;

- the residual angular error does not exceed ±7 mrad at the RFQ entrance;
- the transmission has been computed as a function of the AD beam emittance. No errors have been taken into account as far as potential mismatch between the AD ring and the extraction line is concerned. The results are shown in Figure 13. The transmission is ≈87% for the nominal beam emittance of 1π, while it drops down to less than 80% for the expected initial beam emittance of 5π.

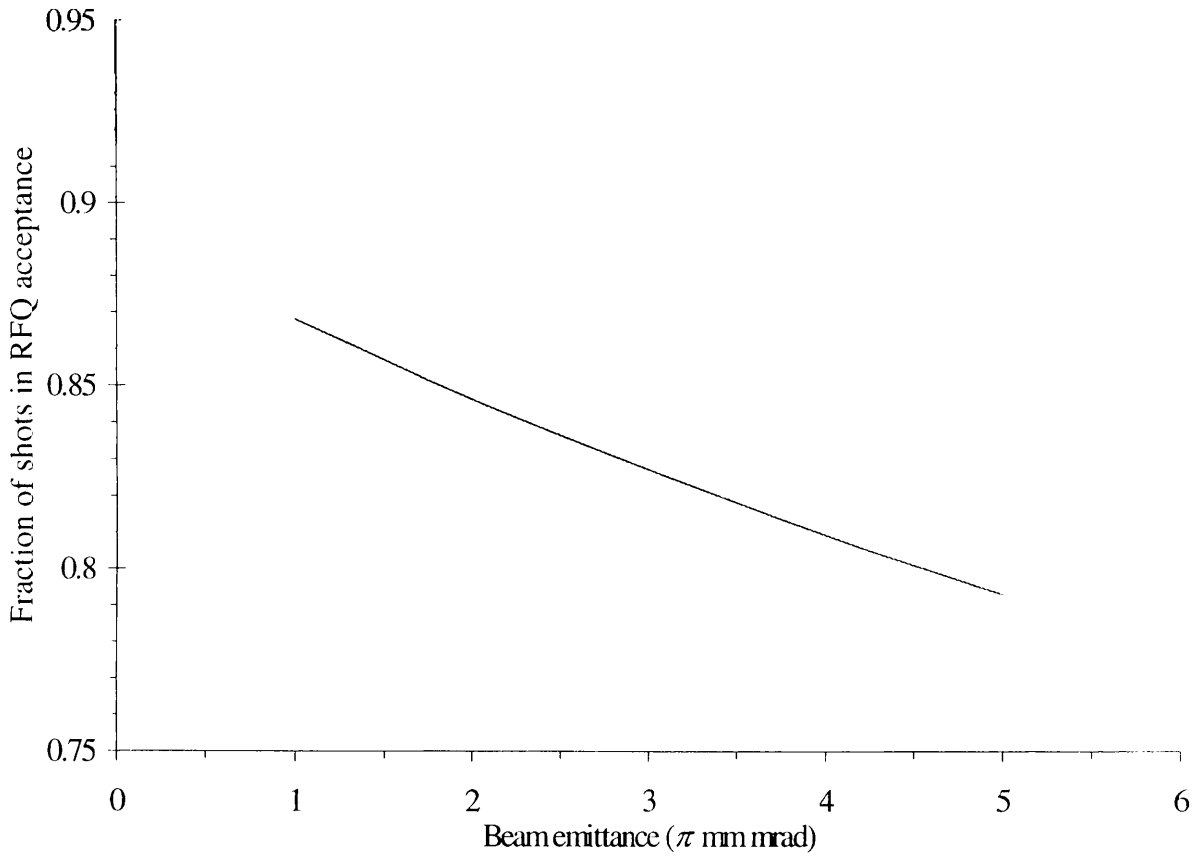

Figure 13 - Fraction of shots within RFQ acceptance vs. AD beam emittance, assuming stability 1×10^{-3} for all individual magnetic elements

It can be concluded from the above plot that the specified overall stability of 1×10^{-3} of the magnetic elements leads to a noticeable fraction of beam shots lost. Superior stability of the active magnetic elements and reduction of parasitic electromagnetic fields is therefore highly desirable.

3.4.2 Low Energy Beam Transport (LEBT)

The purpose of the LEBT is to transport the beam 678 mm from the RFQ output to the vacuum window of the gas-target experiment. The LEBT is composed of 3 existing magnetic quadrupoles (internal diameter 29 mm, external diameter ~113 mm, length 56 mm) placed immediately after the RFQ cover. The schematic layout is shown in Annex B, positions 15, 16

and 17. Position 16, a free space of 150 mm, is reserved for a removable beam diagnostic device.

The beam envelope for an RFQ mid-range output energy of 50 keV is shown in Figure 14. The beam is made parallel after the triplet and it can travel the 440 mm through the diagnostic box to the window without changing substantially in dimension. Similar behaviour has been achieved for the full range of beam energies coming out of the RFQ (approx.10 to100 keV). The beam dimensions at the window are summarised in paragraph 4 (end-to-end simulations)

Existing *magnetic* quadrupoles have been chosen because of their availability. Further studies are foreseen to investigate possible advantages of using *electrostatic* quadrupoles.

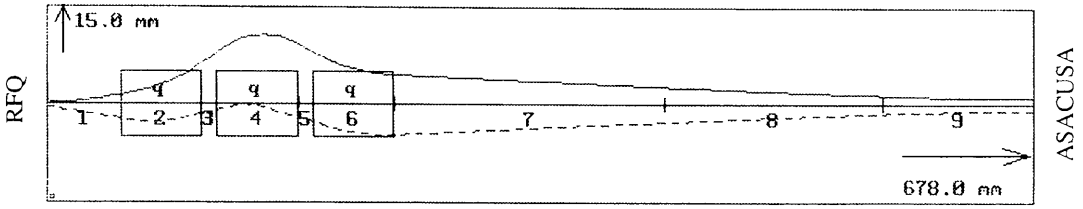

Figure 14 - Beam profiles (radii) in the LEBT for input beam emittance of 1 π
[Top: horizontal plane. Bottom: vertical plane. q= quadrupoles. TRACE results]

3.5 Vacuum System

General considerations

The operational pressure in the RFQ should not exceed about 1×10^{-8} mbar to avoid sparking. With respect to the downstream physics experiments there are two fundamentally different situations:

- *during phase 2* of ASACUSA, the RFQ is at much lower pressure than the experiments. In the worst case the experiment consists of a gas target at about 1 mbar, separated from the LEBT by an ultra-thin formvar window. Sufficient pumping power is provided in the experimental set-up to assure a pressure not exceeding 1×10^{-6} mbar helium at the upstream side of the formvar window. It has been agreed to take this as the standard specification for all experiments of phase 1.

  The pumping power installed in the RFQ has to be designed to assure the RFQ's own operating conditions, taking the gas conductance of the LEBT into due account.

- *during phase 3* the gas flow is reversed since the experiment consists of a cold bore trap imbedded in a superconducting solenoid. This assembly acts as a cryogenic pump that has to be protected from contamination by the RFQ. The latter has to be operated at pressures as low as 1×10^{-10} mbar which implies UHV-compatible design together with corresponding pumping capabilities to absorb outgassing of the walls.

To separate the ASACUSA experiments from the other beam lines, the possibility to install a vacuum window upstream of the RFQ has been studied. Titanium is considered the best material for this purpose because it gives minimum beam straggling for a given mechanical rigidity. But it has been found that even a titanium window as thin as 2 μm would

seriously impair the RFQ performance. It has therefore been decided not to provide such a window but rather to install a fast-acting valve protecting the AD machine from an accidental vacuum break in a beam line.

Slow-acting separating valves are foreseen at the "handover "point at the input of the beam line, as well as upstream and downstream of the RFQ.

Implementation

The layout for phase 2 is determined by the helium flow from the experiment which depends critically on the vacuum conductance of the LEBT. In order to reduce the latter, the RFQ is equipped at its output with a small diaphragm of 10 mm diameter and 2 mm thickness. The LEBT on its smallest aperture consists of a tube of 30 mm diameter and 200 mm length. This geometry leads to a vacuum conductance of 13.4 l s^{-1} for helium as a worst case and hence to a required pumping speed of 1340 l s^{-1}. Turbomolecular pumps are the only type providing reasonable pumping speeds for helium, and such a unit of 1600 l s^{-1} is consequently foreseen.

The layout for phase 3 is determined by the outgassing rate of the RFQ tank which is estimated at 2×10^{-11} mbar l s^{-1} cm^{-2} after 24 hours bakeout at 300 °C. For a limit pressure of 4×10^{-10} mbar the total gas load is then 1.4×10^{-6} mbar l s^{-1} and the required net pumping speed 3500 l s^{-1} hydrogen.

As there will be a baffle and rf shields between the vacuum pumping system and the tank, the effective pumping speed will be reduced by about 50%. It is therefore proposed to use 2 sputter ion pumps of 400 l/s each, together with 4 titanium sublimation pumps (TiSP) of 1350 l s^{-1} each.

A roughing pump is part of the turbomolecular pump assembly. Leak detection will be carried out using mobile devices.

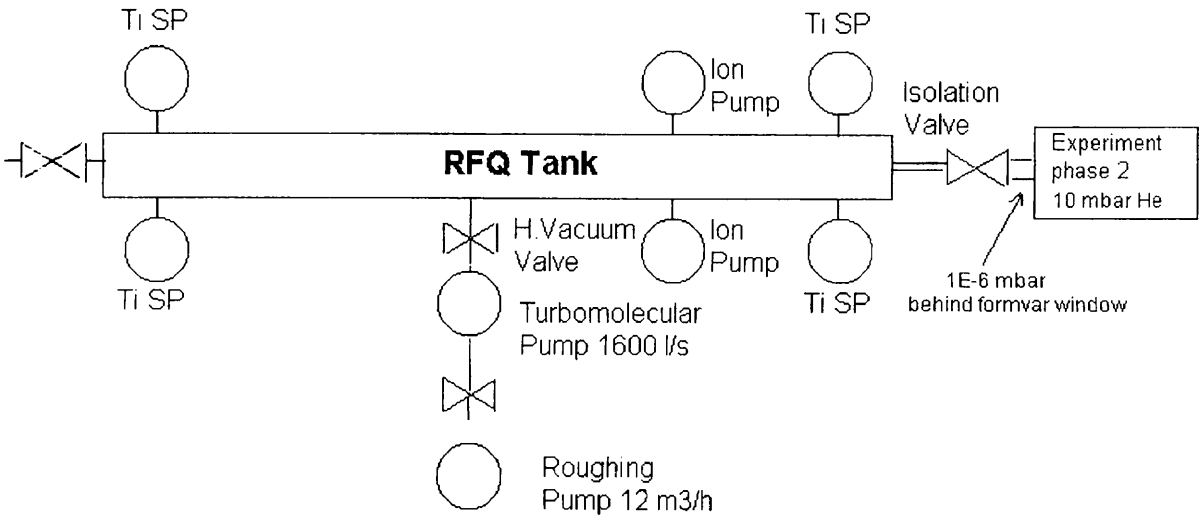

Figure 15 - AD-RFQ Vacuum Layout

3.6 Controls

Hardware

As general controls philosophy, the entire RFQ line will ultimately be operated from a local, or central control room, together with the other elements of the AD machine. The possibility to operate the equipment remotely is also important for the running-in with high-intensity protons, in which case the AD hall is considered as primary radiation area and therefore not accessible.

From a hardware point of view, most of the elements are replicas of modules that are already in operation in other parts of the CERN/PS and, as such, are equipped with standard computer interfaces. Various specific interfaces may exist, e.g. G64 crates with MIL 1553 serial links, but finally all units are equipped to be connected to VME crates (called "DSC") as common front-end concentrators. Local operation for commissioning is in general possible, directly with integrated local controls; "manual" controls via more or less "intelligent" stand-alone equipment could also be considered but would have to be supported by the hardware providers. Local Workstations or X-terminals are available from a pool to cover control needs for the intermediate test phase .

Software

The software to drive standard equipment like power supplies, vacuum equipment, RF equipment etc. is already available in the PS control system and will be used as it is. Only modifications in the database are needed in order to include the additional equipment into the system. New software is only needed for the diagnostic devices. There 2 phases must be distinguished:

- *The R&D phase.* Different detection methods will have to be tried in order to master problems due to the very low beam intensity and due to contaminating particles stemming from the annihilation. During this phase a very flexible system (probably a PC with programs such as EXCEL™ and VISUAL BASIC ™) should be used.
- *The operational phase.* In this phase the detector problems will be solved and the diagnostics should be usable from the control room.

Dedicated programs will be needed for the scintillation fibres. The tasks of histogramming, calculation of beam position, width and integral intensity will have to be covered as well as position calibration and intensity cross calibration with the help of the beam current transformer. For readout of the photo-multiplier signals a new equipment module must be written.

For the scintillation screens an application program already exists. This program must however be adapted to the new environment especially for the non-destructive "watchdog" scintillator with beam hole. The buying of new equipment for video readout, which will need programming effort in order to become operational, has been considered.

4. END-TO-END SIMULATIONS FROM BUNCHER TO EXPERIMENT

In order to take into account a maximum number of beam dynamics aspects, multi-particle simulations have been performed. A uniform beam distribution was generated at the focal point DE1, then transported through all the elements until the end user, i.e. to the thin formvar window for phase 2 and to the middle of the trap for phase 3. The operating parameters were optimised for the precise beam characteristics as specified by the experimenters [ref.1 and subsequent private communications].

The analysis was carried out by the program PARMILA in the beam transfer lines, by PARMTEQ in the RFQ and by PATH in the solenoid area where data of a field map were used for the integration of the particle trajectories. The magnetic field map was provided by the manufacturer of the trap solenoid.

4.1 ASACUSA phase 2 (beam to formvar window)

Table 7 shows the figures for transmission and emittance at the window. It gives the output values for the worst-case "effective overall" input emittance of 10π; a factor 2 less can be expected realistically. It should also be stressed that virtually all the particles are transmitted through the RFQ but only the ones within the energy bracket mentioned below are counted for transmission and emittance evaluation. The transmission is unaffected by the output energy due to the electrostatic post-deceleration.

A histogram of the output energy is shown in Figure 16.

Table 7. Beam parameters at the formwar window

Energy	Transmission (±5 keV)	Total physical emittance	Beam radius	Divergence
100 keV	47%	74 mm mrad	2.8 mm	27 mrad
80 keV	47%	83 mm mrad	2.9 mm	29 mrad
60 keV	47%	96 mm mrad	3 mm	31 mrad
40 keV	47%	117 mm mrad	3.4 mm	34 mrad
20 keV	47%	166 mm mrad	4 mm	41 mrad
10 keV	47%	330 mm mrad	5 mm	66 mrad

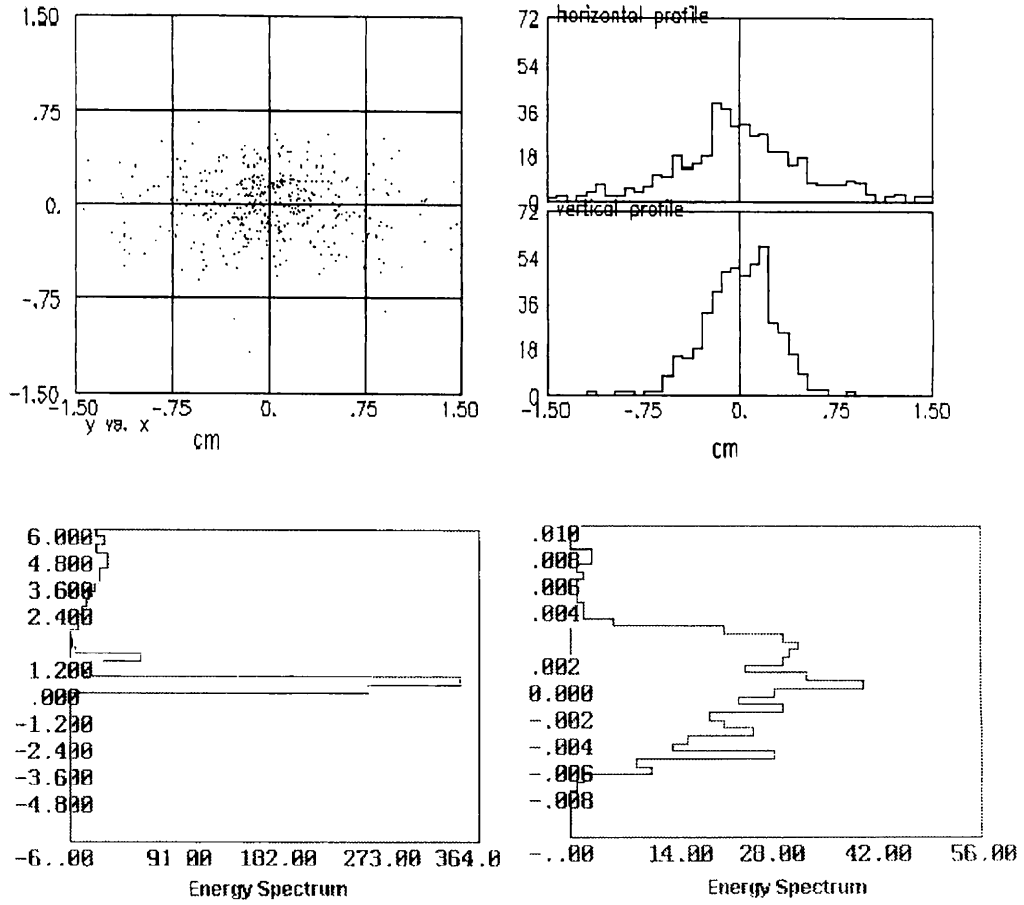

Figure 16 - Transverse space (top) and energy spectrum (bottom) for 50 keV output energy (on a 6 MeV scale, right; on a 10 keV scale, left). (PARMILA results)

4.2 ASACUSA phase 3 (beam to trap in solenoid)

Figure 17 shows the transverse beam profile in the middle of the solenoid.

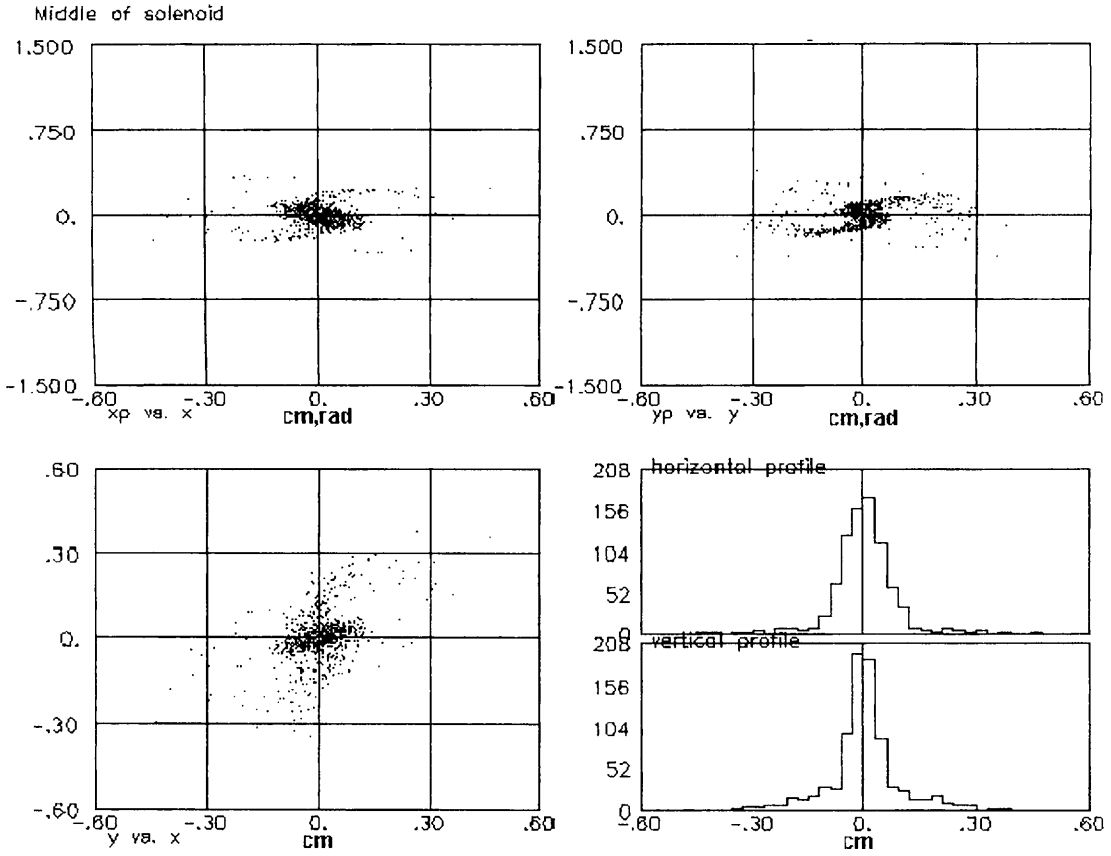

Figure 17 - Transverse phase planes in the middle of the trap (5 Tesla solenoidal field). x (horizontal plane) and y (vertical pland in [cm], xp and yp in [rad]. (PATH output)

Injection conditions have been optimised in order to achieve the minimum spot size and there is no transverse particle loss during the transport to the trap. The overall efficiency of the trap is determined by several parameters: The macro-pulse length, the distance between the RFQ and the trap, the trap length and the energy spread at the output of the RFQ. A trap length of 50 cm and energy spread acceptance of ±5 keV for a 400 ns long macropulse has been defined. The macro-pulse length is determined by the AD bunching system. The time-energy distribution at the output of the AD machine is assumed to be a double Gaussian with standard deviations (σ_t,σ_T) depending on the bunching voltage. Table 8 summarises some of the possible set of parameters and the corresponding number of particles inside the trap acceptance, i.e. the number of particle arriving at the RFQ within 400 ns, and within the RFQ energy acceptance. The full potential transmission of 47% (phase2) cannot be achieved due to the fact that part of the beam lies either outside the RFQ energy acceptance or outside the trap time acceptance.

Table 8. Transmission vs.AD bunching voltage

Bunching voltage [V]	σ_t (ns)	σ_T (keV)	Transmission (DE1 to trap)
20	219	0.5	30%
100	146	1.5	40%
500	97.5	2.3	43%
1000	82	2.7	42%
2500	62.3	3.4	39%

5. DIAGNOSTICS

Design philosophy

The following specific constraints must be taken into account:

- Contamination by annihilation products: The RFQ acts as a very efficient beam transport line in the sense that virtually all protons or antiprotons within the input acceptance are transmitted to the output, albeit only about half of them with the nominal low output energy. While these conditions prevail for adequate alignment of the input beam to the aperture, a misaligned antiproton beam hitting the wall will generate annihilation particles, about three pions/muons for each antiproton lost.

- No test beam at 5.314 MeV is available at CERN.

- The long interval of 70 to 100 seconds between shots makes composite beam measurements tedious, if not impossible. One-shot diagnostic devices such as the "pepperpot" need further R&D for use in a low-intensity antiproton-environment.

- No non-destructive beam measurement methods are available at the low output energy.

General constraints to be added to the list include limited space in the beam line, resolution limits of the low beam signals, interference problems with external light sources and electromagnetic fields, etc.

The impact of these constraints will be minimised by a 4-step approach:

A. Initial Evaluation of RFQ Performance

The RFQ line will be studied extensively, with a beam of known and constant parameters, to commission all components and to verify the key characteristics. One possibility of obtaining a suitable test beam is to transport the entire chain, including power supplies, to a TANDEM generator providing adequate installations, e.g. the Institute of Storage Ring Facilities in Aarhus/Denmark. However, the logistics involved and the cost incurred are serious drawbacks of this approach.

An alternative is the testing with electrons of the same velocity, by scaling particle energy and rf voltage by a factor of 1836. The test set-up consists of an electron source of 5.134 MV/1836 = 2.89 kV, delivering a highly collimated dc pencil beam. The electron beam

intensity has to be limited to about 1 μA to avoid space charge effects. They scale with the same factor of 1836 from the proton limit which is in the mA region for the RFQ. dc currents of this magnitude can be conveniently measured by standard electrometers, using long integration times if needed. This test could be carried out at CERN, probably in the ex-LEAR experimental area.

The electron method will be applied to an existing RFQ with known parameters as proof of principle. The obvious difficulty of handling the extremely low-rigidity beam should be manageable by careful magnetic shielding. In case of convincing results, the method will be used for the AD RFQ, otherwise the transfer to a TANDEM has to be envisaged.

For the electron test a Faraday Cup measuring the beam intensities is foreseen. Polarising the cup will allow an energy threshold to be defined, which distinguishes decelerated electrons from non-decelerated electrons.

In the case of tests with protons and for the final installation the following diagnostic devices are needed:

For upstream beam intensity measurements, a beam (current) transformer "BT" is proposed.

Currently available data for these devices are:

Input charge:	$\sim 1 \times 10^7$ particles (protons or antiprotons)
Output charge:	$\sim 5 \times 10^6$ particles
Present resolution:	$\pm 2 \times 10^6$ particles
Resolution that can be reasonably expected with moderate improvements over today's techniques:	$\pm 1 \times 10^6$ particles

The BT would be used in all 4 phases.

Better resolution may be obtained by a different technique under development at present [3]. Figures will be available in about 4 months from now, once a prototype is measured.

For profile measurements we propose to use optical methods. Scintillation - fibres, protected from external light sources by a thin (a few hundred Á) Al layer may be used. Scintillation screens with digital readout are the alternative. In this case it is important that the TV camera observes the screen at an angle of 90 degrees in order to avoid problems with parallax. Development of special In/Out mechanisms may be needed.

Pin diode strip lines may be used if they prove to be compatible with vacuum requirements.

Scintillation screens or scintillation fibres, although mainly targeted at profile measurement, may also be used for intensity measurements when calibrated with a beam current transformer. It is important to be able to measure the ratio of decelerated to non-decelerated beam. In the absence of a spectrometer one might consider 2 consecutive calibrated scintillator screens of different thickness, where the first will intercept all low energy particles and the second will measure the particles not captured by the RFQ rf and thus passing the device with their initial energy.

Another idea may be time-of-flight measurements downstream of the RFQ. After a drift of ~1m the non-trapped beam would be separated from the decelerated beam. A Faraday Cup, calibrated scintillation fibres, or a scintillation screen may be used for relative intensity measurements. The Faraday Cup should work well for protons. For antiprotons, however, it is unclear how much of the charges stemming from annihilation products will be lost. Also the differing energies of the particles to be measured may cause problems.

B. Provision to Attach Removable, Destructive Beam Diagnostics

Provisions are foreseen to introduce destructive diagnostics in the beam lines, for full beam measurement during commissioning or during interruptions of operation.

Upstream of the RFQ the beam-spot may be measured by a scintillator screen. The image can be digitised and beam spot parameters like position and transverse beam width can be extracted. Alternatively, scintillation fibres may be used.

Table 9 shows the list of beam monitors foreseen upstream of the RFQ:

Table 9. Retractable measurement devices to be installed in the beam line

Description	Comments	Resolution [mm]	Acceptance [mm]	Availability
monitor 1	multi-proportional wire chamber	1.0-2.0	16.0-32.0	yes
monitor 2	profile measurement (Scintillator/watchdog 1)	0.5	15.0	no
monitor 3	profile measurement (Scintillator/watchdog 2)	0.5	15.0	no

The resolution of the existing multi-proportional wire chamber can be easily changed by the replacement of a control card. The profile measurement monitors will use scintillator screens or fibers, mounted on in/out mechanisms of proven design. They will be housed in the same box and use the same readout equipment as the "watchdog" scintillators (see paragraph C below)

Downstream of the RFQ a short rudimentary low-energy beam transport (LEBT) with a T-section will be permanently installed where devices like scintillator crystals or Faraday cups may be introduced.

C. Operational Non-destructive Beam Diagnostics

It can be safely assumed that an input beam delivered within the RFQ acceptance is transmitted with nominal efficiency to the output, since on the one hand the inherent properties of the RFQ are given by its electrode design and are known to be constant, on the other hand the rf parameters of the amplifier chains are servo-controlled and can be precisely verified.

A permanent BT and two annular "watchdog"-scintillators are foreseen upstream of the RFQ. The former measures the received intensity. The latter are void of any obstruction in the centre and intercept only the particles outside the nominal acceptance of the RFQ.

These three elements together permit complete, if rudimentary, monitoring of the beam delivered to the RFQ. On the basis of the data obtained it can either be concluded with high confidence that a beam with acceptable parameters has been produced at the output, or on the contrary that some anomaly of quantifiable parameters was the reason for a probable failure.

D. Diagnostics of the physics experiments

Diagnostics such as beam intensity monitors are integral part of the experiments. They are the ultimate judge of the overall AD and RFQ performance. Calibration runs during the commissioning phase will be necessary to relate their results (based on destructive beam measurements) to the data from upstream instrumentation (taken by non-destructive transmission methods).

All these components together will provide a post-mortem analysis of each beam pulse and shall allow, with due experience, diagnosis and corrective action of irregularities should they occur.

6. ADAPTING THE AD FOR THE RFQ

The RFQ poses more demanding requirements on the quality of the beam from the AD than experiments that use a degrader foil to stop the 100 MeV/c antiprotons. Tight tolerances in angle and position of the beam at ejection have to be observed in addition to the small beam *emittance*. To meet these requirements, it is essential to have very good closed-orbit control and high stability of the main magnets and the extraction- and correction magnets at low momentum. In addition, the beam energy has to be controlled to better than 10^{-3}, which poses tight tolerances both on the electron cooling system and on the rf of the ring.

A simulation from the last turns in the ring to the entrance of the RFQ should be completed so as to establish the tolerances on the ring elements in more detail. Also during the commissioning, deeper detailed studies will be done on the stability and reproducibility of different elements.

7. PROJECT SCHEDULE

The general planning of the project is shown below.

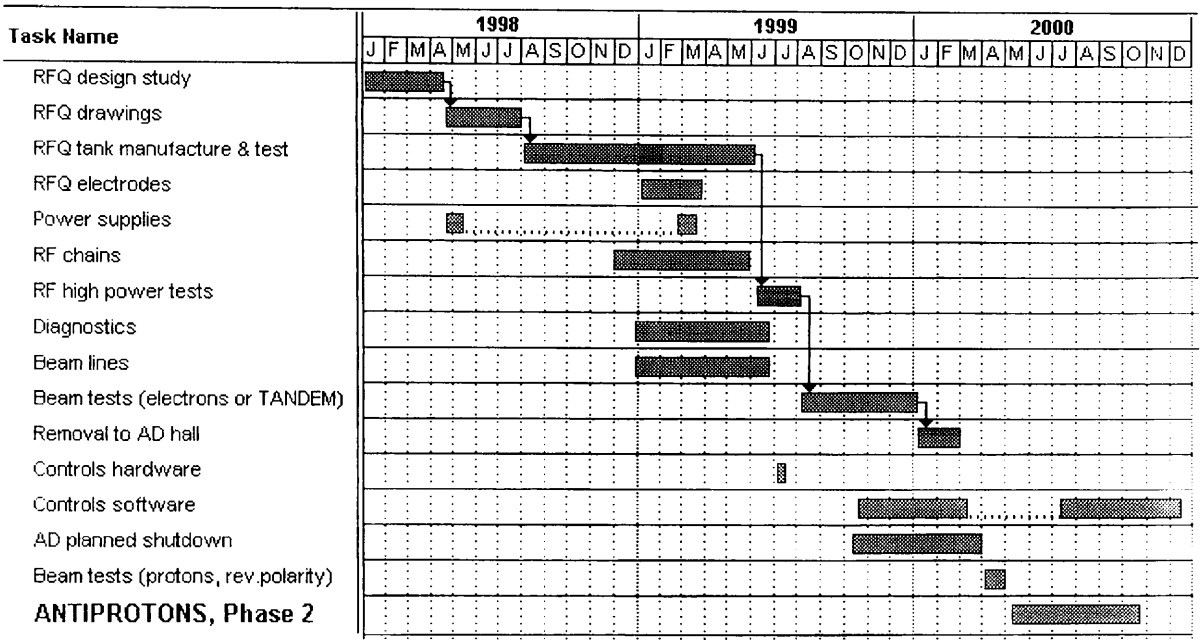

The sequence of tasks has been arranged to permit the start of ASACUSA phase 2 as soon as the AD machine permits, namely beginning of May 2000. This date is determined by the planned AD shutdown and the scheduled tests using protons (with bending magnet fields reversed to allow circulation of particles in the correct direction).

The critical element is the heavy equipment for the RFQ. Detailed technical design has to start by January 1998 to allow elaboration of the manufacturing drawings and subsequent construction of the tank and its accessories. The planned duration of hardware tests with high-power rf is reduced in favour of the beam tests, to allow a maximum of information -gathering even in case the time-consuming transfer of the whole line to a Tandem machine for tests would be necessary.

The electrodes for the RFQ are not on the critical path and definition of their precise profile may be delayed until spring 1999 to accommodate refinements as a consequence of further beam dynamics studies in 1998. Manpower requirements for the beam lines, diagnostics and rf equipment are however more important than initially estimated and necessitate external support for timely termination of the project (see also Section 8 below).

The schedule is based on the assumption that the project is approved no later than the month of May 1998, when the fully-fledged set of production drawings has to be ordered. The mechanical engineering studies are already being carried out on the basis of an interdivisional CERN agreement, anticipating the approval. Another key milestone is the start of the RFQ tank manufacture in August 1998 for which adequate funding must be ready.

8. ESTIMATED COST AND MANPOWER

Estimations for cost and CERN manpower of the different subsystems is summarised below.

Cost is given in terms of 1997/98 Swiss Francs and comprises two parts:

- Column 1 concerns the procurement of all new material and/or the refurbishing of CERN provided items, as well as cost of external temporary labour to complete the system.

- Column 2 gives estimated "hardware" value of items provided by CERN free of charge, as in-kind contribution to the project. Examples are the rf power amplifier or the elements of the MEBT. These elements are part of the strategic reserve of CERN and available only in very limited quantities. It should also be emphasised that the replacement cost of these elements would be considerably higher.

The individual cost estimates have been rounded up in increments of 5 kCHF. No other contingencies are included.

Manpower , expressed in man-years, concerns two categories:

- Column 3 lists the requirements for the design, implementation and commissioning of the project which can only be covered by CERN personnel. Replacement by external support is NOT possible.

- Column 4 lists the *additional* manpower needs that can be covered by external help (on CERN site) or collaborations (at home institutes). Prior commitments of the different groups for other projects, including the AD machine, do not permit full CERN participation in the critical years 1998 and 1999. External support is therefore mandatory if the project shall be carried out as outlined in Section 7 (Project Schedule).

Grand Total:

The overall cost of the project amounts to 1.780 million Swiss Francs and the total manpower requirements to 8.8 man-years for the construction phase during the years 1998 to 2000. Adequate resources for the subsequent operation have also to be foreseen, in accordance with the general AD operation and maintenance management.

In case the RFQ commissioning tests have to be carried out with protons from a Tandem machine outside CERN, the removal and logistics costs of about 40 to 80 kCHF and 0.5 man-years have to be added to the above.

	Cost [kCHF]		Manpower [MY]	
	CERN procurements	CERN in-kind	CERN	External
RFQ structure	300		0.4	
Buncher and energy corrector cavities	35		0.1	
RF equipment	420	200	0.5	
Power supplies (HV, MEBT)	60		0.2	
Beam lines				
- upstream (MEBT)	60	100	0.4	
- downstream (LEBT)	60	30	0.1	
Vacuum system	95		0.2	
Controls (hardware, software)	65		1.1	
Diagnostics (operational items)	120		0.5	1.0
Infrastructure in AD hall	65		0.1	
RFQ measurements				
- special diagnostics (+R&D)	50			1.0
- test setup	50		0.5	
Upgrading of the AD for the RFQ	50		0.2	
Miscellaneous (incl. project management)	20		1.5	1.0
TOTAL	**1 450**	**330**	**5.8**	**3.0**

9. ACKNOWLEDGEMENTS

The continued inflow of information from the ASACUSA team, especially Y. Yamazaki, the spokesman R.S. Hayano, and the contact man J. Eades is gratefully acknowledged. Very useful contacts to the physics community were established by R. Landua. Thanks go also to M. Doser, M. De Saint-Simon and M. Pullia for their presentations concerning specialised aspects of the project.

10. REFERENCES

[1] T. Azuma et al., "Atomic Spectroscopy And Collisions Using Slow Antiprotons", ASACUSA Collaboration, (Spokesman: R.S. Hayano), CERN/SPSC 97-19, CERN/SPSC P-307 (1997).

[2] S. Baird et al. "Design study of the Antiproton Decelerator: AD", (Editor: S. Maury) CERN/PS 96-43 (AR), 1996.

[3] F. Pedersen, private communication.

The following computer programs have been used to prepare this report:

- MAFIA (CST Gesellschaft f. Computer Simulationstechnik).
- PARMILA, PARMTEQM, PATH, POISSON, TRACE, (Los Alamos National Laboratory, USA).
- PSPICE (MicroSim).
- MAD (CERN).
- PROJECT98, WORD95 (Microsoft).

APPENDICES

A.- Layout of the overall system

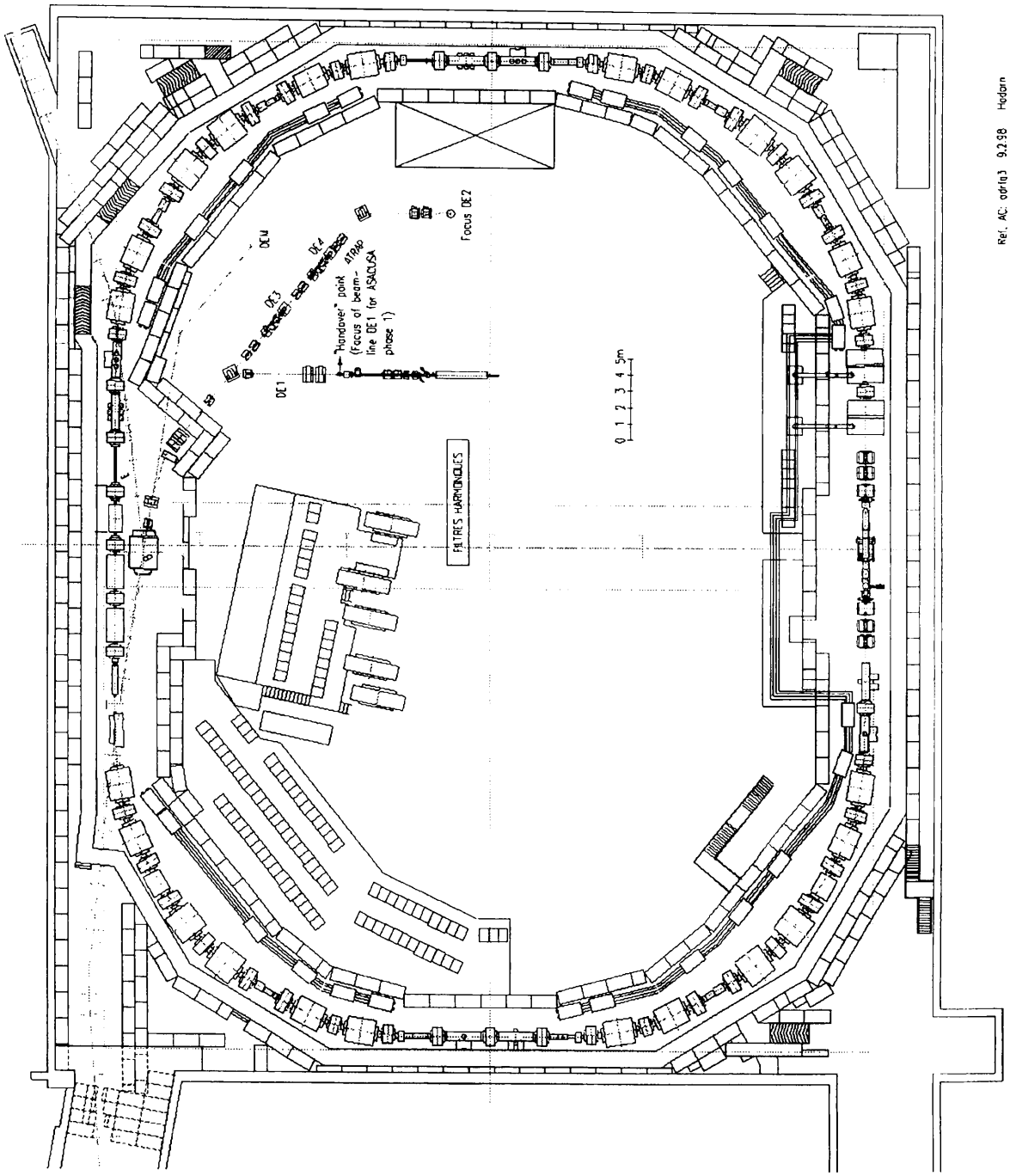

B.- Details of the RFQ

LEGEND:

#	Designation	Mid-position [mm]	Length [mm]
1	Buncher	0	300
2	Beam transformer	450	~ 400
3	Manual vacuum valve	780	75
4	Wire chamber	1145	404
5	Vacuum chamber (removable)	1920	1360
6	Quadrupole no. 1	3052.5	560
7	Quadrupole no. 2	3692.5	560
8	H/V steerer no. 1	4237.5	350
9	H/V steerer no. 2	4784.5	350
10	Scintillator/watchdog no. 1	5059.5	200
11	Scintillator/watchdog no. 2	5594.5	200
12	UHV vacuum valve	5746	103
13	Energy corrector	5947.5	300
14	RFQ	7857.5	3520
15	Low-energy beam transport (LEBT)	9711.5	188
16	Diagnostics (optional)	10065	150
17	UHV vacuum valve	10191.5	103

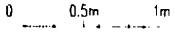

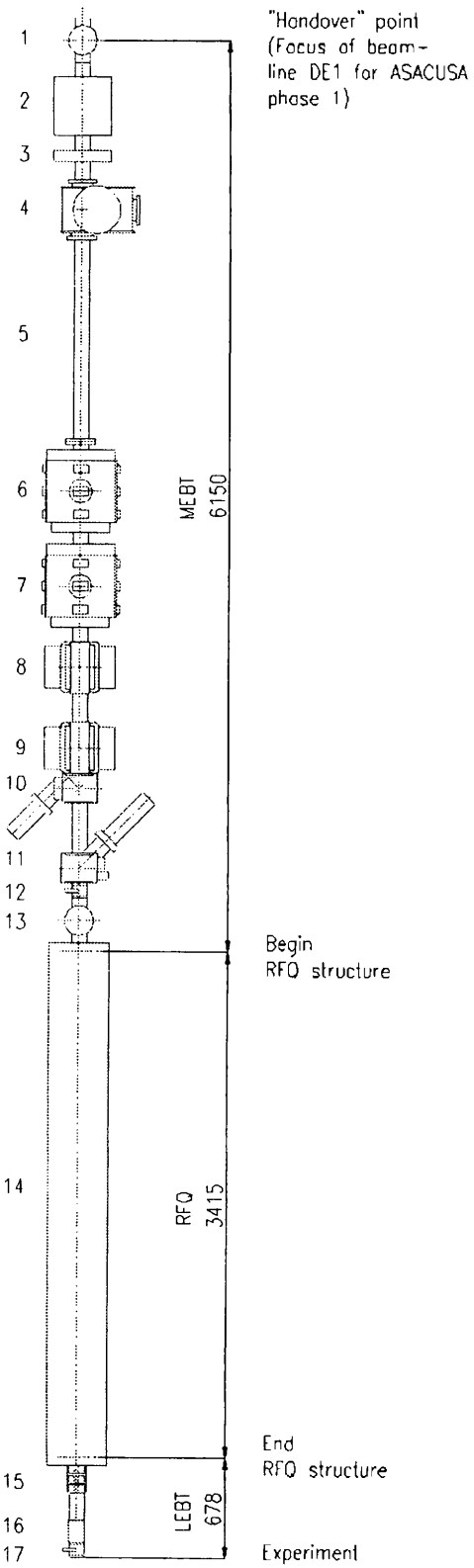

C.- Other considered solutions

Five solutions have been studied and proposed for the RFQ. The abundance of solutions comes from the request of energy variability, at least for the first phase of the experiment, in a range as-wide-as-possible around 50 keV. The RFQ itself cannot provide energy variability, and so other RF elements have to be added to the system. The configurations considered are the following and a sketch is shown in Figure 16 :

1. "Evolution of the fixed energy solution": RFQ to 80 keV then double gap buncher. Energy variability 10-130 keV.

2. "It's easier to accelerate than to decelerate": RFQ to 50 keV and acceleration with temporary equipment to be removed in phase 2. Energy variability: 40-80keV.

3. "5.314 MeV to 10 keV is too big of an excursion for one frequency". High-energy section at 200 MHz, Low-energy section at 100 MHz. Transition around 400 keV. Energy variability: 10-140, 300-500 keV

4. Use to our advantage the "entrance Problem". The RFQ tank would be divided into two sections independently powered and phased, the second one with flat electrodes. The first part of the RFQ would decelerate the antiprotons down to keV energies, and the potential drop between the wall of the second cavity and the electrodes would provide the energy variability.

5. Electrostatic solution presented in this paper, for comparison.

The important output beam characteristics for the five solutions are presented in Table 9.

Table 9. Comparison of the five versions studied in detail

		Transmission at 50 ± 10 keV	Emittance at 50 ± 10 keV	Output energy range	Remarks
1.	RFQ + buncher with "symmetric" acceleration/deceleration	40%	180/106 mm mrad	10-130 keV	
2.	RFQ + buncher mainly for acceleration	46	150/113	40-80 keV	
3.	Double frequency 200/100 MHz	42	150/110	10-140,300-500 keV	Longer drift length required, 1 extra rf cavity needed
4.	RFQ + small rfq	(41% at 80 keV)	(200/145)	80-130 keV	Minimum output energy 80 keV
5.	RFQ with electrostatic acceleration/deceleration	46	150/113	0-100 keV	CHOSEN SOLUTION

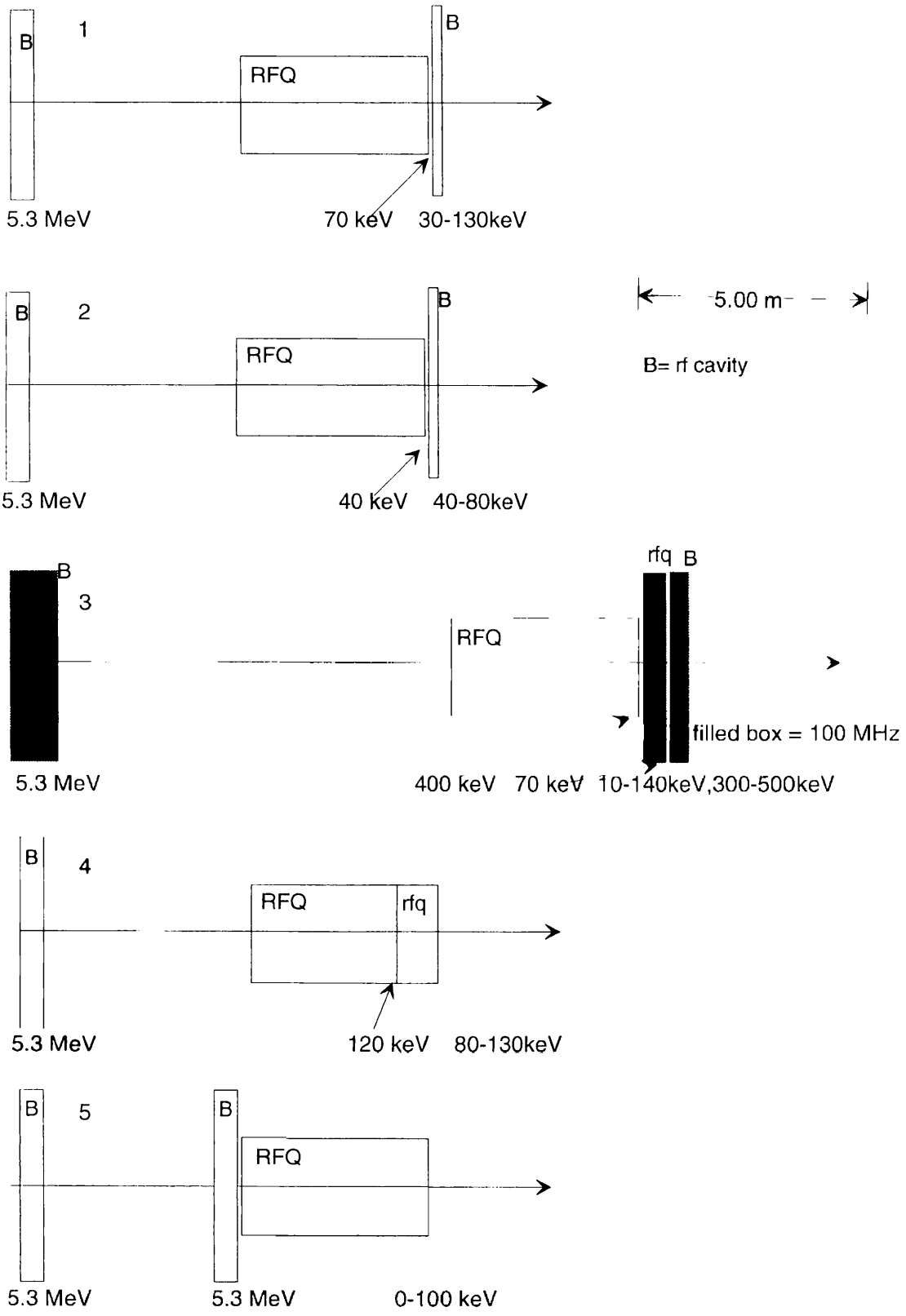

Figure 16 - Schematic layout of the five configurations studied in detail

D.- The ASACUSA experiment

(contributed by J. Eades)

It may be useful to add a few lines here concerning the ASACUSA project, as it is the ASACUSA collaboration that has asked PS Division to construct the RFQ discussed here, with funds drawn from the SHINPRO budget. These funds were guaranteed by the Japanese science ministry in February 1997, but will only become available from 1/4/98. The ASACUSA proposal was approved on Nov 20th by the Research Board, which recognised the essential nature of the RFQ for the second and third phases of the proposed series of experiments, using keV rather than MeV antiprotons. The Research Board therefore decided to discuss the scientific programme of these later phases once outstanding technical questions concerning the RFQ have been settled.

The installation of equipment for the first (non- RFQ) phase of ASACUSA will take place as soon as the experimental hall is ready in 1998; this phase is essentially a continuation of the PS205 LEAR experiment. It uses a 1 Bar, low temperature helium target completely isolated from the 5.314 MeV AD beam line by a short air path following a ~100 micron window at the end of the beam pipe.

These experiments should be terminated by 2000, at which time ASACUSA will switch to the low pressure target required for work with keV antiprotons. In addition to extending laser spectroscopy work to low pressure (1-10 Torr) targets, phase 2 will investigate atomic interactions of antiprotons in the keV or tens of keV energy range using similar gas pressures. The latter experiments represent an extension of research previously carried out at LEAR by PS194. The low-energy domain of both PS205-like and PS194-like experiments can only be reached with a post-decelerator and the only serious candidate for such a post-decelerator is an RFQ. Moreover, the PS194-like experiments require a variable energy output beam from the RFQ. As the low energy beam need only be delivered into a target vessel, the requirements on its emittance are not stringent. In practice, however, the use of such ultra-low energies means that the experiment is no longer completely isolated from the beamline (i.e. from the RFQ). In the `swarm' type of experiment the low-energy antiprotons will enter a pumped target vessel attached to the end of the RFQ. The target gas, helium at 10 mTorr in the worst case for pumping, will be retained in an appendix within this vessel by a 0.3-0.4 micron formvar window. In the 'dE/dx' type of experiment there will be no window at all; the target will be at the centre of a vacuum chamber of some 40 cm in diameter, and will consist of mTorr pressure noble-gas jets, or of thin foils. In both types of experiment, pumps will maintain the target vessel walls at a sufficiently low pressure to be accommodated by the RFQ.

Seen from the beam line, phase 3 experiments resemble closely PS196 and PS200 at LEAR, and ATHENA and ATRAP at the AD, in the sense that the RFQ output will be collected in a trap operated at very high vacuum. The variable energy will not be needed, and it should be possible to isolate the experimental apparatus downstream of the trap from the beamline/RFQ by valving off the trap once the antiprotons are inside.